ADVANCED MATERIALS
www.advmat.de

Mixed Ionic–Electronic Conduction, a Multifunctional Property in Organic Conductors

*Siew Ting Melissa Tan, Aristide Gumyusenge, Tyler James Quill, Garrett Swain LeCroy, Giorgio Ernesto Bonacchini, Ilaria Denti, and Alberto Salleo**

Organic mixed ionic–electronic conductors (OMIECs) have gained recent interest and rapid development due to their versatility in diverse applications ranging from sensing, actuation and computation to energy harvesting/storage, and information transfer. Their multifunctional properties arise from their ability to simultaneously participate in redox reactions as well as modulation of ionic and electronic charge density throughout the bulk of the material. Most importantly, the ability to access charge states with deep modulation through a large extent of its density of states and physical volume of the material enables OMIEC-based devices to display exciting new characteristics and opens up new degrees of freedom in device design. Leveraging the infinite possibilities of the organic synthetic toolbox, this perspective highlights several chemical and structural design approaches to modify OMIECs' properties important in device applications such as electronic and ionic conductivity, color, modulus, etc. Additionally, the ability for OMIECs to respond to external stimuli and transduce signals to myriad types of outputs has accelerated their development in smart systems. This perspective further illustrates how various stimuli such as electrical, chemical, and optical inputs fundamentally change OMIECs' properties dynamically and how these changes can be utilized in device applications.

1. Introduction

"Smart systems" where sensing, logic, actuation, energy harvesting/storage, and information transfer are performed locally and autonomously have great potential in impacting major sectors of society including the internet of things (IoT), healthcare, and energy. Within the more traditional microelectronics community, this need has led to the advancement of myriad technologies such as microchips designed for low-power consumption and sensing as well as high-energy-density batteries for energy storage. Recently, interest in developing systems that interface seamlessly with the human body (e.g., wearables, brain–computer interfaces, and soft robots) has driven the development of soft, organic, and biomimetic materials that emulate the functions of their inorganic counterparts. Beyond emulation, these materials are unique because they provide an opportunity to embody such multifunctional properties within the material itself, rather than relying on device design. These multifunctional properties are intrinsic to organic mixed ionic electronic conductors (OMIECs), that is, once synthesized and processed, OMIECs can serve as the active component of multiple devices (be it transistors, sensors, energy-storage devices, etc.), where essentially the material is the device.

OMIECs generally consist of a conjugated backbone for electronic conduction as well as sidechains to facilitate ionic intercalation from the operational electrolyte and to aid in solvation in processing solvents.[1] Organic chemistry provides a large toolbox in the molecular design of the backbone, side chains, and other additives, resulting in an almost infinite design space for the corresponding materials properties: energy levels, electronic and ionic conductivity, optical, volume, and moduli. Additionally, one or more of these properties can be modified during device operation, thereby transducing an input (e.g., ionic) into an output (e.g., electronic), allowing OMIECs to be used for a variety of applications including sensors, transistors, optoelectronic devices, energy-storage electrodes, and actuators. The multifunctionality of OMIECs is illustrated in **Figure 1** to highlight their versatility in design and their ability to respond to a variety of stimuli.

The underlying and unifying phenomena behind these property changes arise from the large modulation in electronic and ionic charge density in the bulk of the OMIEC. This modulation in turn results in second-order effects such as modulations in electrochemical potential (electron energy levels), electronic and ionic transport, capacitance, free volume, optical bandgap, and modulus. Tuning these properties throughout the bulk of the material enables new design parameters that were previously untapped in traditional electronic devices where

S. T. M. Tan, A. Gumyusenge, T. J. Quill, G. S. LeCroy, G. E. Bonacchini, I. Denti, A. Salleo
Department of Materials Science and Engineering
Stanford University
Stanford, CA 94305, USA
E-mail: asalleo@stanford.edu
G. E. Bonacchini
Center for Nano Science and Technology @PoliMi
Istituto Italiano di Tecnologia
Via Giovanni Pascoli, 70/3, Milano 20133, Italy
The ORCID identification number(s) for the author(s) of this article can be found under https://doi.org/10.1002/adma.202110406.

DOI: 10.1002/adma.202110406

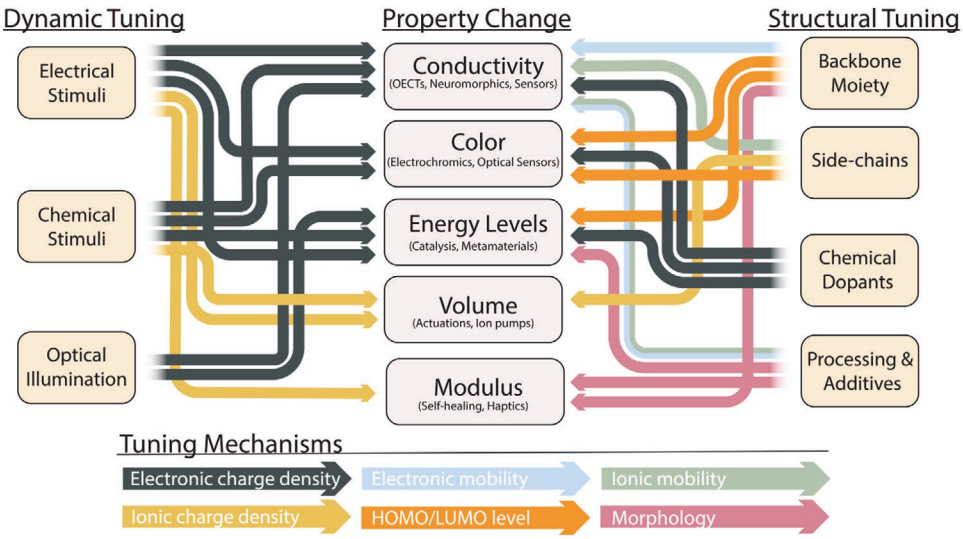

Figure 1. Multifunctional property tuning in OMIEC materials. The schematic illustrates how various device relevant properties can be dynamically tuned or intentionally designed into the structure of the material as well as the mechanism by which the specific property is modulated. For example, adjusting the electric potential of a device can dynamically alter the conductivity of an OMIEC by changing the charge carrier density in the material (top left). On the other hand, substitution of different backbone moieties into the structure of the material will also alter the conductivity by changing the carrier mobility in the OMIEC (top right). Similar relationships are shown for different dynamic and chemical (static) tuning methods and various properties. The mechanisms by which properties are modulated are shown at the bottom of the schematic.

typically electrical or optical modulation occurs at interfaces. For instance, the ability to tune charge density throughout the bulk results in large volumetric capacitances, activating thickness as a tunable parameter to optimize transconductance of a transistor, in addition to channel width and length. Additionally, the permeability of chemical species throughout the bulk improves reactivity for sensors and fuel cells without the need for physical nanostructuring of scaffolding electrodes. Uniquely to OMIECs, and hence the underlying theme of the current discussion, this tunability can be achieved in a single material making the design and synthesis of novel OMIECs a hot topic as of recent. Devices including organic electrochemical transistors (OECTS),[2] electrochromic displays (ECDs),[3] actuators,[4] neuromorphic transistors,[5,6] bioelectronic devices,[7] and more,[1,8] thus exploit such modulation in OMIECs for different applications. With some of these technologies already approaching commercialization,[9] a comprehensive understanding of their operating mechanism is crucial to bridge the disconnect that exists between the fields of molecular design and synthesis, device physics, and device manufacturing.

This perspective highlights the various approaches to tune the ionic–electronic properties in OMIECs. We classify them either as structural—chemical modifications during materials design and preparation—or dynamic property changes during device operation. We aim to showcase the uniqueness and richness of these materials both chemically and technologically, as a single material can be utilized in different device architectures owing to the functionality that is physically embedded in its bulk and afforded via mixed ionic–electronic conduction. We first discuss how structural tuning (such as polymer backbone and sidechain engineering) can be used to co-design novel materials for specific devices. This section aims to inspire synthetic and materials chemists to revisit design principles that are crucial for marrying ionic and electronic conduction in a single material system. We then provide an overview of how the properties of a material are tuned during device operation (dynamic tuning) to uncover the working mechanism for each property change. Last, we discuss key property changes in OMIECs as well as resulting technologies. Throughout this perspective, we aim to provide an outlook on research opportunities on repurposing existing materials and/or designing new materials and devices. We thus hope that this perspective will inspire collaborations between materials and device engineers as the multifunctional nature of OMIECs requires an equally multidisciplinary team of chemists, materials scientists, as well as electrical, chemical, and mechanical engineers to design next generation materials and devices to fully harness their potential.

2. Structural Tuning

Conjugated polymers are by far the most widely studied class of OMIECs and will thus be the focus of our discussion. One can simplistically assume that to design a high-performing OMIEC, tethering ionically transporting sidechains onto existing excellent electron- (or hole-) transporting backbones (as represented in **Figure 2**) would suffice. However, such a task has shown to be more complex as ionic insertion, resulting in bulk swelling, and concomitant property changes are rather complex and warrant more careful materials considerations. Furthermore, sidechains affect the self-assembly of the material, which in turn determines its properties. To uncover the structural tunability of polymer mixed ionic–electronic conductors (MIECs), we will discuss backbone and sidechains engineering as separate design strategies, but readers are reminded that in practice, both from a synthetic and an engineering point of view, these two cannot be decoupled especially at the microstructural

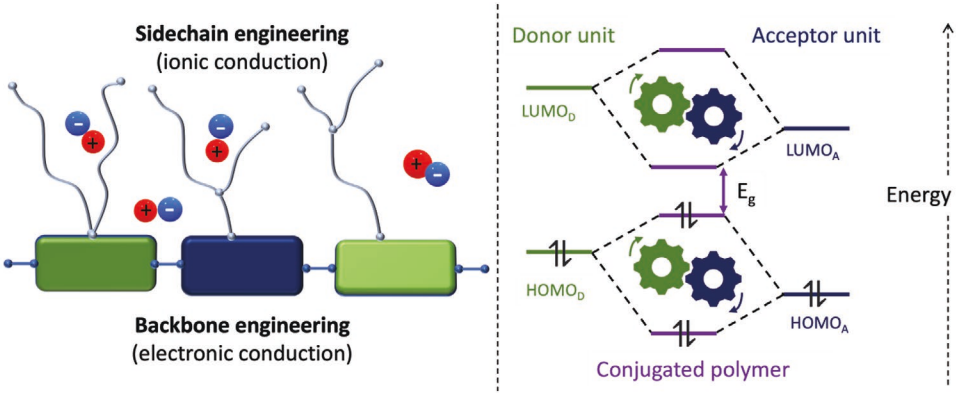

Figure 2. Schematic representation of two major structural considerations for designing a polymeric MIEC. For the sake of a simplified discussion, ionic transport is attributed to sidechains and electronic transport to the conjugated backbone. In practice, sidechains serve as ion shuttles/hosts into the film and concomitant charge generation and delocalization occur along and between conjugated backbones. Also shown is the energy diagram in conjugated polymers showing the tunability of the energy bandgap via fine structural tuning of donor (D) and acceptor (A) units.

level. We focus on homo- and copolymeric OMIECs as the discussion on heterogenous blends. Other notable classes include blends and copolymers of electronic and ionic conductors (e.g., PEDOT:PSS).[1]

2.1. Backbone Engineering

Backbone engineering in polymer MIECs has benefited from recent advances in polymer chemistry, wherein, for the past four decades, major milestones have been reached in terms of extending conjugation lengths, tuning charge carrier delocalization as well as substituting heteroatoms along polymer backbones. To uncover the design principles of OMIECs, let us begin with a simplistic chemical structure of an all-acceptor polymer such as a poly(alkoxythiophene) (PAT).[10] The conjugated core consists of a thiophene ring, on which alkoxy groups are anchored. The sulfur atom (heteroatom) allows tuning of the electron density within the core. More (or less) electron-withdrawing atoms (O: furan, N: pyrrole, Se: selenophene) can be used to tune electron densities, molecular planarity, and π–π interactions. Though most of the reported polymer MIEC structures are thiophene-based, heteroatom substitution is still a viable route toward designing new OMIECs. For instance, the backbone planarity afforded by increasing the radius of the heteroatom has yet to be fully investigated in combination with efficient ionic conduction. The energy distribution across the ring allows different reactivities, which are commonly exploited for polymerization and for aromatic substitutions at different positions on the conjugated ring. Such reactivity can be utilized for the synthesis of fused-ring systems,[10] an area that has yet to mature in OMIECs. Molecular fine-tuning of the core unit and the substituting groups constitutes a large field of study in polymer chemistry beyond this discussion.

A commonly studied example of PATs is poly(3,4-ethylenedioxythiophene) (PEDOT) where the building block is slightly electron deficient due to the presence of oxygen atoms. More importantly, the bridged substitution obviates the regio-irregularity possibility (along with minimized twisting along the backbone), making PEDOT and its derivatives one of most studied classes of redox-active organic materials. Though the homopolymerized and hole-transporting (or p-type) EDOT derivatives remain more studied, the tunability presented by its simple yet rich structure opens avenues for the design and synthesis of more complex backbones. For instance, the copolymerization of the functionalized dioxythiophene unit with efficient charge-transporting building blocks was recently shown to be an effective route toward donor–acceptor polymers with excellent performance in OECT devices.[11] Further tuning of electron affinity along the conjugated core has also yielded electron-transporting polymer MIECs (n-type polymers).[9,12–15] The most widely studied group of n-type OMIECs consists of a naphthalenediimide (NDI) core, which is often copolymerized with a more electron-donating building block (e.g., unsubstituted thiophene). In such an electron-depleted π-conjugated core, electrons have shown to be effectively injected and delocalized along the polymer chain especially when ionically conductive sidechains are utilized.[12,16] The complementarity afforded by utilizing electron-transporting polymers and hole-transporting counterparts has recently become of great interest in OMIECs especially for polymer-based energy storage.[13] Though n-type OMIECs remain underexplored in comparison to their p-type counterparts, recent efforts have demonstrated that outstanding device performances can be realized especially via backbone fine-tuning. However, further efforts are still warranted on this front specially to address: i) poor backbone planarity (commonly introduced by the bulky NDI unit), ii) environmental instability found in most n-type polymers, not to mention iii) boosting their electronic mobilities which still lag behind those demonstrated in p-type counterparts. The balance of electron density along the core thus remains a key approach for controlled modulation of energy levels, the coloration of the chromophores, as well as the molecular packing for tunable ionic intercalation, some of the key tunable properties in OMIECs which are discussed in later sections.

2.2. Sidechain Engineering

In polymer MIECs, sidechains play a key part in the unique nature of these materials, that is, not only do they serve as

solvating media for the electrolyte, but also as: i) molecular shuttles for ionic species in and out of the bulk, and ii) key components in the crystallization and packing of polymer chains. As previously introduced, polar sidechains are commonly utilized in OMIECs mostly to enable ionic intercalation (Figure 2). In some cases, sidechains have also been used to directly dope the polymer backbone.[12,16] It is thus evident that their design/selection is a key aspect in electrochemical devices. Since sidechain engineering will impact several of the properties that are impacted by backbone engineering, in the later sections we will only discuss those properties that seem less intuitive and those that are unique to sidechain modification. Recently, emerging mixed-ionic conducting polymers have been designed without sidechains such as the ladder polymer poly(benzimidazobenzophenanthroline). While this class of materials is out of the scope of this perspective, readers are directed to reviews by Torricelli et al.[8] and Che et al.[17]

2.3. Chemical Doping

When other synthetic approaches (e.g., backbone and side-chain engineering) are undesirable, chemical doping of OMIECs can be an effective method for altering the "native" state of the material.[18] Common chemical dopants are small molecules that are either highly electron-rich or electron-withdrawing to facilitate electron-transfer reactions between the OMIEC and dopant. For instance, electron-rich dopants with amine moieties such as 4-(2,3-dihydro-1,3-dimethyl-1H-benzimidazol-2-yl)-*N*,*N*-dimethylbenzenamine[19] and triaminomethane derivatives[20] are highly effective electron donors to electron-conducting n-type OMIECs. Electron-deficient dopants such as 2,3,5,6-tetrafluoro-7,7,8,8-tetracyanoquinodimethane (F4TCNQ) extract electrons from shallow highest occupied molecular orbital (HOMO) p-type OMIECs, increasing hole concentration. The resulting increase in charge density improves conductivity for a variety of devices such as transistors and thermoelectric devices (see Section 4.2.1). Additionally, the change in Fermi level and electrochemical potential of electrons can alter the OMIEC's subsequent reactivity to other redox-active species in the environment (see Section 3.2) as well as their optical properties. This ability to alter the initial state of material provides even more space to tune the properties of OMIECs for a particular application, as the initial state (i.e., the position of the Fermi level in the density-of-states) of an OMIEC can be shifted such that the range of conditions over which an OMIEC exhibits dynamic response in conductivity, color, and energy levels can be tuned for an arbitrary range of stimuli.

2.4. Processing & Additives

OMIEC micro- and nanostructure (morphology) impacts all aspects of material performance, including charge-carrier mobility, kinetics of device operation, and mechanical/chemical stability.[21] Broadly, the necessity of coupled ionic and charge-carrier motion in OMIECs is thought to require materials that have largely disordered, amorphous regions that facilitate rapid ion transport while simultaneously having well-connected, ordered domains that facilitate charge-carrier transport. These conflicting requirements have made it so that the optimal morphology for OMIECs is still an active area of research. Design strategies highlight the vast number of tunable controls that exist in both material synthesis and processing.[22,23]

Control of the morphology and nanoscale interactions of OMIECs not only dictates electronic properties, but also dictates mechanical properties. In polymeric MIECs, mechanical properties such as modulus, breaking strength, and elastic limit are intimately linked to the size, distribution, and amount of crystalline aggregates in the material. For example, controlling these aggregates has led to the development of seemingly "rigid" (i.e., high-modulus) polymer semiconductors that display remarkable flexibility and maintain electronic transport properties by inducing nanoconfinement of the polymer and reducing aggregate size.[24] These developments have long-reaching applications in biosensing, flexible thermoelectrics, and even artificial skin.[25] This further shows that understanding material microstructure is not only of fundamental interest, but is also of immense practical importance, as microstructure impacts properties seemingly as disparate as electronic and mechanical properties. Such complexity in the microstructure of OMIECs thus complicates the fundamental understanding of device operation. During OMIEC operation in electrochemical transistors for example, significant volume expansion occurs concomitant with disruption to the ordered regions due to penetration of ions into the bulk during the volumetric charging process.[26] Furthermore, the exact nature of interaction between penetrating ions and the OMIEC is poorly understood. Recent studies have suggested that glycolated sidechains in polymer OMIECs can chelate around ionic species, leading to significant film morphology disruption.[27] Ultimately, design rules governing the optimal morphology for OMIECs remain fertile ground for investigation. It is expected that the future deployment of operando and in situ characterization techniques will facilitate the development of such design rules.[28] In particular, techniques such as X-ray scattering combined with electrochemical measurements could elucidate the complex dynamics which arise during charging, many of which are still relatively unknown. Additionally, spectroscopic techniques including visible and infrared absorption spectroscopy and Raman spectroscopy provide insights into both ordered and disordered domains of these materials, although detailed modeling is often required to link these changes back to the OMIEC structure.

3. Dynamic Tuning

Dynamic changes in the properties of OMIECs enable them to respond to and transduce external stimuli into a variety of output signals. Changes in electronic and ionic charge density are the unifying phenomena behind modulations in its electrochemical potential, conductivity, color, modulus, and volume as illustrated in **Figure 3**. Modulation in charge density can be induced by a variety of external stimuli such as electrical impulses, exposure to chemical species, or under the influence of optical illumination. The increase in electronic charge density on the conjugated backbone results in changes in electrochemical potential (Fermi level), conductivity, and optical

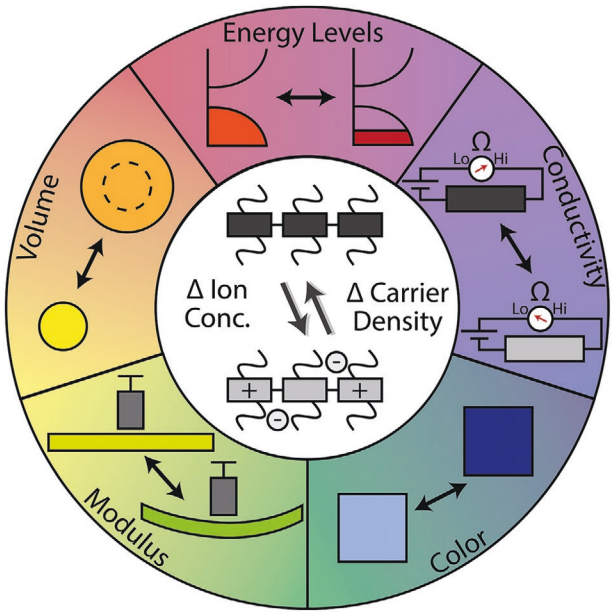

Figure 3. Dynamic tuning of OMIECs. The unifying phenomena underlying changes in OMIECs' properties are charge density. Accumulation of electronic charges on the OMIEC's backbone increases electronic carrier density which results in changes to electrochemical potential (electron energy levels), electronic conductivity, and color. The simultaneous increase in compensating ion concentration reduces elastic modulus and increases volume.

bandgap. During operation, the OMIEC is typically immersed in a medium containing solvated ions (solid or liquid electrolyte). As the electronic charge density changes on the OMIEC's backbone, counterions are transported between the OMIECs' matrix and the electrolyte to ensure electroneutrality. This further influences the ionic conductivity, modulus, and volume of the OMIEC. With the myriad sources of stimuli—electrical, chemical, and optical—that modulate the charge density of OMIECs, which subsequently result in a variety of changes in materials properties, OMIECs can be utilized for a variety of devices that comprise intelligent autonomous systems—sensors, energy harvesting/storage, logic, memory, actuation, and communication.

3.1. Electrical Stimuli

OMIECs can be deposited on the surface of electrically conductive planar substrates (such as in sensors, thermoelectrics,[29] electrochromics,[30] and electrochemical actuators[31]) or as a conductor between two electrodes (e.g., channel material of transistors[2]). Sources of electrical inputs can range from external electronic circuits (such as the operation of thermoelectrics, ion pumps,[32] transistors, electrochromics, and actuators) or from biological sources (such as single cells, tissues, organs, and other physiological or aqueous environments). By applying an electric field or potential on the OMIEC, electrons or holes can be injected capacitively into the lowest unoccupied molecular orbital (LUMO) or HOMO (n-type or p-type, respectively), thereby increasing the OMIEC's charge density. Though electrically stimulating OMIECs on different surfaces has been widely shown, chemical and mechanical mismatch between the softer (and often hydrated) OMIECs and common electrodes remain major challenges. Engineering the Young's modulus of the materials, mitigating the corrosion and oxidation at the metallic interfaces are crucial to ensuring better electrical performances. This is thus a potential area of study for future applications, especially for long-term implantation and biointerfacing. Bimetallic material or metallic alloys, carbon nanotubes, graphite, and highly reactive biodegradable metallic fillers,[33–35] among other strategies are potential electrode candidates.

3.2. Chemical Stimuli

Another common approach to tune the charge density of OMIECs is via their interaction with chemical species in the environment. OMIECs can interact with chemicals in a variety of processes such as faradaic charge transfer from redox-active molecules and capacitive interactions with ions. Instead of applying an electric potential, charges can be accumulated in the OMIEC via faradaic reactions from redox-active molecules in the OMIECs' environment. Depending on the relative electrochemical potential of electrons on the OMIEC and the chemical species, oxidizing or reducing agents can be utilized to extract or inject electrons into the OMIEC. As noted above, applying a potential on an OMIEC dynamically tunes the electrochemical potential of electrons, thereby controlling the relative reactivity of the OMIEC to the reactant. Judicious design of sidechains on the OMIEC enables favorable interactions with molecules in its environment. For instance, the recent development of polar sidechains using glycol moieties enables the intercalation of hydrophilic or polar species throughout the bulk of the OMIEC electrode, allowing for volumetric reaction and charging.

Achieving effective charge transfer between the analyte and OMIEC requires appropriate alignment of the electrochemical potential of electrons on the OMIEC electrode and the redox species. Failure to do so may result in the subsequent transfer of charges to other redox-active sinks in the environment, leading to undesirable side reactions and products that may interfere with the OMIEC's operation. Electrons flow from a region of higher to lower electrochemical potential. Hence, achieving electron transfer from redox-active species to the OMIEC requires the latter to have a deep LUMO (high electron affinity). Alternatively, chemically p-doping the OMIEC to first deplete the HOMO could subsequently allow the filling of the HOMO by the redox-active species (see above for structural tuning). On the other hand, electrons can be transferred from the HOMO to the redox active analyte, thereby oxidizing the electrode. It is challenging to utilize electron-conducting polymers with low-lying LUMOs for direct electron transfer as the high electron energy in the LUMO may result in the subsequent loss of electrons to ambient oxidative species such as molecular oxygen.[36] Due to their ability to volumetrically solvate ions from the operational electrolyte, OMIECs are also ideal materials to detect the concentration of ions in aqueous analytes. The OMIEC's potential varies logarithmically with the concentration of ions in solution according to the Nernst equation. This potential can be measured directly against a reference electrode or second-order

effects resulting from this change in potential can be recorded (such as electronic conductivity in OECTs). Therefore, OMIECs are commonly used as electrodes for ionic sensors to detect Na^+, K^+, Mg^{2+}, Ca^{2+}, NH^{3+}, and other ions commonly present in physiological solutions.[37,38] To ensure specificity, the OMIEC can be functionalized with synthetic[38] or biological membranes[39] that selectively allow some ions to permeate. Furthermore, OMIECs can also be functionalized with ligands that bind to non-redox active and neutral molecules where the binding of these analytes could increase the impedance, optical properties, or pH of the electrode.[40] The ability to function in aqueous electrolytes and detect a variety of chemical inputs makes OMIECs ideal material candidates in long-term health[41] and environmental-monitoring devices.[42]

The accumulation of holes by the oxidation of p-type OMIECs or the accumulation of electrons by the reduction of n-type OMIECs after exposure to redox-active species can result in changes in electronic conductivity, such as in the channel of an OECT.[43] When a chemically sensitive OMIEC gate is used, the change in potentials on the gate are coupled capacitively to the channel's potential. Hence, chemical changes occurring on the gate during sensing directly influence channel conductivity. For instance, the presence of lactate secreted by cells grown on an OMIEC gate resulted in amplified current signals across the channel.[44] Caution should be taken when conducting these faradaic reactions in the presence of applied electric fields in electrochemical devices as they may affect the reaction rates in unexpected ways and accelerate parasitic side reactions and chemical degradation of the OMIEC.[45] An alternative approach would be to separate the processes of chemical detection and conductivity modulation.[46]

On the other hand, during the sensing of ion concentration, the intercalation of ions from the electrolyte increases the ionic conductivity and volumetric capacitance of the OMIEC. This reduces the OMIEC's impedance, which can be measured by electrochemical impedance spectroscopy. Simultaneously, the change in potential of the OMIEC from ions in solution influences the electronic charge density and hence conductivity of the OMIEC. Therefore, electrolyte-gated transistors[8] are a common architecture used to transduce these ionic concentration changes into drain-current modulations. Since these ions are not redox-active within the potentials typically applied in OMIEC-based devices (sub 1 V), these capacitive (or potentiometric) devices do not encounter issues faced by the faradaic chemical sensors. Faradaic charging of the OMIEC in an aqueous electrolyte results in simultaneous uptake of ions from the electrolyte and swelling of the OMIEC material. Hence, electrochemical actuators can be powered by OMIECs functionalized with enzymes to catalyze the reaction of metabolites such as glucose, enabling self-powered artificial muscles.[47] Harvesting energy from the environment to power soft actuators opens potential applications in smart stimuli-responsive soft robots and microfluidic valves.

3.3. Optical Illumination

The conversion of optical stimuli into electrical signals has been largely exploited for numerous applications, from biomedical sensing to optical communication, imaging, night vision, thermal efficiency analysis, and flexible optoelectronics.[48–51] Compared to the above forms of stimulation (i.e., electrical and chemical), utilizing optical illumination to dynamically tune the properties of OMIECs in devices is yet to be explored. This opens opportunities for investigating OMIEC-based analogs of typical device configurations such as solar cells, phototransistors,[52] and photodiodes for biocompatible and low-voltage operation.

Moreover, besides these conventional electronic platforms, light-sensitive OMIECs could potentially play a role in the development of optoelectronic interfaces for neurostimulation. Indeed, traditional hydrophobic organic electronic materials have recently emerged as opto-bio actuators in both in vitro and in vivo applications, where photoexcitation effectively modulates the biological activity of cells and tissues.[53–56] While the physical and physiological mechanisms of stimulation in these systems are often not fully elucidated,[57,58] the phototransduction mechanism is generally associated with thermal effects, charge-transfer reactions (Faradaic coupling), photochemical phenomena, and capacitive coupling at the biotic/abiotic interfaces.[59,60] In fact, a common strategy to increase photostimulation relies on materials configurations that maximize the effective electrochemical surface, such as nanostructured planar interfaces,[61,62] nanoparticles,[63] or hierarchical nanocrystals.[64] This seems to suggest that although little is known on whether OMIECs can play a role to further advance this emerging field, their ability to establish strong capacitive couplings through volumetric charging—along with their synthetic tunability and biocompatibility, which mirrors that of traditional organic semiconductors—should be taken into consideration for future developments of optoelectronic biointerfaces.

In a similar way, the emergence of organic photoelectrodes[65,66]in photocatalytic and photoelectrochemical applications can inform design strategies for OMIECs. While these devices have conventionally utilized traditional organic semiconductors that are hydrophobic, analogies can be drawn to design OMIECs with photoactive properties. This represents yet another opportunity for OMIECs, where their intrinsic redox-activity could be further enhanced by means of photocatalysis.

4. OMIEC Property Changes

Having provided an intuition on how different structural modifications and dynamic stimuli can be utilized to modulate the properties of OMIECs, we shift our focus on understanding the physical and chemical meaning of key property changes and on discussing various device technologies enabled by such changes. We discuss both chemical (static) and stimuli-responsive (dynamic) techniques for modulating energy levels, conductivity, coloration, and volume to demonstrate the utility of OMIECs. For each property, we will cover mechanistic implications which should be considered when employing such tuning methods, and touch on the crossover between methods where relevant. We will also discuss device demonstrations enabled by each property change and highlight future research opportunities with a special emphasis on modulating different properties in a single material system.

4.1. Energy Levels

4.1.1. Chemical Tuning of Energy Levels

The location of the HOMO and LUMO (or valence and conduction band) of an OMIEC is heavily influenced by the chemical structure of the polymer backbone. More thorough summaries of the synthetic approaches for tuning the energy levels of semiconducting polymers are available elsewhere,[67] but useful intuition regarding tuning of the HOMO and LUMO levels can be garnered by a simplistic particle-in-a-box analogy. The introduction of electron-donating (or withdrawing groups) will increase (or decrease) the HOMO and/or LUMO levels of the material as shown in Figure 2. In this respect, the sidechains grafted onto the polymer backbone will in fact affect the energy levels in the material, as the substitution of alkyl versus glycol sidechains can introduce different resonance and inductive effects. However, for efficient ionic transport, glycol sidechains (or a blend of alkyl and glycol chains) are desired,[23,68] meaning that most practical methods for energetic tuning include employing different backbone moieties and heteroatom substitutions. Further energetic control can be achieved by adjusting the conjugation length of the polymer and limiting the number of repeat units over which the charge can delocalize—shorter conjugation lengths will widen the bandgap. Conjugation length can be limited via the insertion of conjugation breaks (e.g., thieno[2,3-b]thiophene) into the backbone of the polymer[69] or from intra-ring torsion due to steric effects[70] and extended by promoting backbone planarity through the introduction of bridging units or by non-covalent interactions between adjacent rings which promote coplanarity.[71–73]

Functionally, there are many situations where it is desirable to synthetically tune the energy levels of an OMIEC, but they largely revolve around adjusting the stability of charges, which are injected onto the polymer backbone. In the field of organic bioelectronics, p-type materials with an ionization potential below 4.9 eV or n-types with an IP > 4 eV afford OMIECs stable operation in water and other biocompatible environments by avoiding parasitic side reactions.[12,36] The offset between the HOMO of the cathode, and the LUMO of the anode also dictates the operating potential of OMIEC-based polymer batteries.[13,74] Analogous to electrochemical stability, the HOMO/LUMO levels of OMIECs can also be tuned to optimize these materials for catalysis or faradaic chemical reactions, where band height and alignment is needed for reactions to proceed.[36]

Chemical dopants can also be used to control the initial energy levels of electrons in these material systems when other synthetic approaches may be undesirable. The relative electrochemical potential (energy level) of electrons on the OMIEC with that of redox-active species in the environment can result in charge-transfer reactions between the OMIEC and the chemical species. These reactions may be desirable, such as those used during chemical sensing (faradaic) of a target analyte, or undesirable, such as the oxygen reduction reaction (ORR) with ambient molecular oxygen. For instance, to increase the stability of electrons to minimize ORR side reactions, p-type dopants such as the high-electron-affinity F4TCNQ that extract electrons from the HOMO of p-type OMIECs can be added.

Morphology also plays a crucial part in setting the energy levels of OMIECs. Extensive work on conjugated polymers has shown that the optical bandgap can be tuned by inducing structural order/disorder in solid-state films via control of processing solvent, material molecular weight, and even device temperature. This is largely due to the sensitivity of the HOMO and LUMO energy levels to the effective conjugation length in conjugated polymer OMIECs. Furthermore, this sensitivity of the HOMO/LUMO levels to material microstructure holds for a wide variety of polymeric materials, including the prototypical polymer poly(3-hexylthiophene) (P3HT) and more recent material developments in donor–acceptor copolymers.[75] The ability to correlate HOMO/LUMO levels with microstructure provides a sensitive probe to understanding structure, and the ability to control structure provides a powerful tool to tune material performance, with applications ranging from ECDs/windows to novel sensors and thermoelectric devices.[76,77]

4.1.2. Tuning Energy Levels Dynamically

Besides the chemical approach of intrinsically changing the location of an OMIEC's energy levels, these can also be tuned during device operation. This is exemplarily manifested when OMIECs are utilized as energy-storage electrodes. During charging, an external voltage is applied across the two electrodes, thereby injecting electrons in the LUMO of the n-type conductor and holes into the p-type conductor. This increases the electrochemical potential of electrons on the anode and decreases that on the cathode, thus storing charges as potential energy that can be released upon connection with a load. Counterions from the operational electrolyte simultaneously intercalate into the electrodes for electrostatic compensation. As OMIECs are simultaneously redox-active and iono-electronically conductive, neither additives nor binders are required unlike in conventional energy-storage technologies (e.g., lithium-ion batteries). Furthermore, they can be operated in safe aqueous electrolytes, enabling applications in biological environments including implants, wearables, and lab-on-chip devices making harvesting of chemical energy from the environment realistic. The OMIECs' sidechains further enable solvation in processing solvents, allowing the extraction of the active materials from current collecting electrodes at the device's end of life followed by redeposition onto fresh electrodes for a new lease of life. These properties enable ease of recycling of OMIEC electrodes for the circular economy of organic electronic technologies.[74] Additionally, the energy levels can be modulated during the faradaic (charge transfer) reactions we discussed above between OMIECs and redox-active analytes. Such reactivity has recently enabled self-powered implants and wearable devices that obtain energy from biological fluids,[78] an emerging field and a platform for future studies on how electronics interface with living organisms. Besides the electrochemical approaches, illuminating the OMIEC with pulses of light is also another route for exciting electrons to higher energy levels to be subsequently transferred to the desired oxidant such as in photoelectrochemical cells used for sensing or water splitting.

4.2. Conductivity

4.2.1. Chemical Tuning of Conductivity

Strategies to increase the electronic conductivity of semiconducting polymers predominantly rely on increasing the charge carrier mobility of holes or electrons for p- and n-type materials, respectively. High charge-carrier mobility is largely enabled by charge delocalization along the polymer backbone (intrachain transport) aided by chain-to-chain hopping (interchain hopping) when charge carriers meet chain ends or other morphological traps (e.g., sharp kinks). Efficient charge delocalization is commonly associated with backbone coplanarity, conjugation length, narrow bandgaps, and high degree of order between chains. Though such strategies are commonly effective in other electronic devices such as organic field-effect transistors (OFETs), their relationship with device performance remains an emerging field of study in electrochemical devices. Here, the polymer backbone must accommodate incoming ions and their transport must be optimized concomitantly with electronic transport.

In OECT devices where electronic conductivity often serves as an important figure of merit, a few of the aforementioned backbone engineering strategies have shown to translate to improved device performance. For instance, the effect of backbone conformation on device performance was probed by comparing a triethylene glycol (TEG)-bearing benzo[1,2-b:4,5-b′]dithiophene (BDT) homopolymer to its thiophene (T) and 2,2′-bithiophene (2T) copolymers.[79] BDT was selected to afford a rather linear homopolymer while the copolymerization tunes the backbone curvature. This strategy showed to result in: i) tunable backbone orientation relative to the substrate, ii) controllable ionization potentials, and iii) increased polymer crystallinity, which ultimately translated to improved conductivity. In fact, a 100-fold increase in transconductance was observed when the homopolymer was compared to the copolymer derivatives in respective OECT devices. Record-high performance could further be realized when electron-rich building blocks were utilized to tune the sidechain distribution as well as the film swelling. Other parameters include efficient polaron delocalization along the polymer chain,[80] as well as operation stability.[79] When designing novel OMIECs, the relationship between the proposed structure and the resulting solid-state behavior must be probed for combined electronic and ionic transport. Demonstrating high carrier mobility (electronic conductivity) alone becomes insufficient, especially if no new insights are gained on how the ionic uptake into the polymer bulk impacts the generation and delocalization of electronic charges. Ideally, one should target the generation of many yet highly mobile carriers in the bulk to achieve excellent modulation of an OMIEC.

One of the unique hallmarks of OMIECs is volumetric doping of the material, enabled by the large free volume of polymers and ionically conductive sidechains, which facilitate counterion motion throughout the bulk of the material.[1] It is this ability to modulate the bulk conductivity that separates OECTs from more conventional thin-film transistors and gives rise to the large values of normalized transconductance, which make these OMIEC materials attractive for many applications. In this regard, the sidechains of the material do not contribute to electronic conduction but are wholly responsible for the ionic conduction and the volumetric doping of the material. The most commonly employed strategy for engineering ionic conductivity into OMIECs is replacing the alkyl sidechains from conventional organic semiconductors (OSCs) with polar oligoethylene glycol sidechains.[23] The choice of sidechains in polymeric OMIECs has been shown to dramatically impact material morphology and OMIEC performance. Specifically, the ubiquitous choice of glycolated sidechains generally leads to materials with more disordered microstructures, improved ionic transport, and decreased electronic charge-carrier transport compared to analogous alkylated versions of the same materials.[23] Furthermore, the design of glycolated sidechains can be tailored with different lengths, branching points, and densities to simultaneously change ion and charge-carrier transport properties.[23] More recently, it has been demonstrated that blends of alkyl and glycol sidechains can be desirable for OMIECs, as these sidechain blends can counterbalance electronic mobility, device stability, self-assembly, and volumetric doping.[13,16,81] As previously mentioned, the sidechains play a crucial role in microstructure formation in OMIECs, and consequently, even minute adjustments to sidechain length, polarity, or density can lead to pronounced differences in resulting properties.

Although less studied than in traditional organic semiconductors, chemical doping of OMIECs can be employed to enable highly tailored materials properties. Just as in more conventional OSCs, doping of OMIECs typically involves redox reactions between dopant molecules and the material, resulting in a shift of the Fermi level. Such reactions will modulate the carrier concentration in the material, resulting in a change in conductivity. This allows one further control over the "native" state of the material, where conductivity can be either enhanced or diminished, depending on the specifics of the system. Such strategies can be very useful in practical applications such as biosensors, where aligning the peak transconductance of the material to the electrochemical potential range of interest can lead to improved response and sensitivity. Similarly, in many electronics and bioelectronics applications, molecular dopants have been used to shift the threshold voltage of devices, thereby increasing the resistance of the material in its native state to enable low power operation. An excellent example of changing material conductivity was shown by the chemical de-doping of PEDOT:PSS in which the operating mode of electrochemical transistor devices was altered from depletion mode, where the material is initially doped prior to stimulus, to enhancement mode, where the material is initially de-doped.[18] Additionally, increasing charge-carrier density and mobility is important for increasing power factor and electronic conductivity in thermoelectric devices as shown in **Figure 4**. Recently, the incorporation of polar glycol sidechains in OMIECs improved the solubility of dopants in the OMIECs (for example F4TCNQ for p-type polymers), lowering required dopant concentrations, thus minimizing the disruption of the OMIEC's microstructure.[82]

Though the relation between conductivity (both ionic and electronic) and OMIEC morphology is a complex and still-evolving area of research, semiconducting polymers have shown to perform efficiently thanks to the presence of tie-chains, that is, less ordered regions can be bridged by long chains to enable

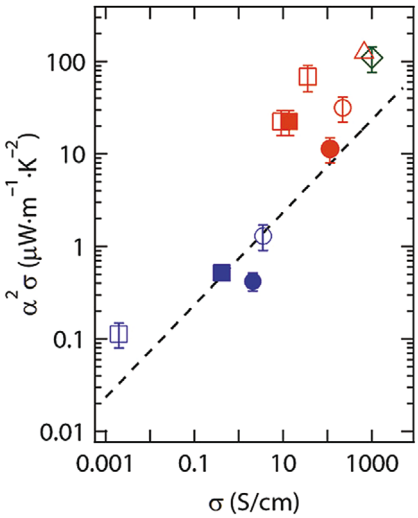

Figure 4. Power factor versus electronic conductivity of PBTTT films chemically doped with F4TCNQ (circles) and F2TCNQ (squares). Reproduced with permission.[77] Copyright 2017, The Authors, published by American Association for the Advancement of Science. Reprinted/adapted from ref. [77] © The Authors, some rights reserved; exclusive licensee American Association for the Advancement of Science. Distributed under a CC BY-NC 4.0 license http://creativecommons.org/licenses/by-nc/4.0/.

efficient charge transport.[83,84] This behavior becomes a promising venue for electron transport to be married with ionic transport as the latter is favored in less ordered systems. Microstructure engineering thus becomes important to realize morphologies that simultaneously favor ionic uptake and efficient electron delocalization. The morphology of OMIECs is heavily influenced through processing by choices of solvents, cosolvents, material blend ratios, and processing post-treatments. Extensive work on P3HT showed that the quality, size, and number of ordered domains, and thus the resulting charge-carrier mobility, could all be controlled by careful selection of the solvent/cosolvent.[85,86] A similar idea has been applied to the prototypical OMIEC, PEDOT:PSS, where choice of cosolvent and/or solvent additives for the aqueous PEDOT:PSS has been extensively studied.[87,88] Aqueous PEDOT:PSS is commonly mixed with a low volume fraction of ethylene glycol, as this is thought to produce more well-connected ordered domains that improve charge mobility while not disrupting ionic transport significantly. Crosslinking agents and acid post-treatments to PEDOT:PSS have also been explored as methods to tailor film morphology and transport properties.[89,90] Ultimately, materials chemical design (i.e., backbone and side-chain design) must be studied alongside appropriate materials processing design, as the resulting performance of OMIECs is closely linked to the final material microstructure.

4.2.2. Dynamically Tuned Conductivity

The ability to dynamically tune the charge density throughout the bulk of OMIECs results in large changes in their conductivity, which has been exemplified by OECTs.[91,2] The electrical polarization of an OMIEC in presence of mobile ionic charges results in significant modulations of the hole (or electron) carrier density within the material. The unique mixed transport properties of this class of polymers give rise to capacitive charging effects that involve the entirety of the materials' bulk, effectively establishing volumetric capacitances ranging from few tens to hundreds of F cm^{-3}.[92,93] These remarkable capacitance values exceed those displayed by electrical double-layers, as well as those achievable with state-of-the-art high-permittivity dielectrics.[91] As a result, charge-carrier density variations of many orders of magnitude are obtained with sub-volt polarizations (exceeding 10^{20} cm^{-3}),[94–96] enabling low-powered switching devices.

In efforts to unravel the complex relationship between materials characteristics and device physics, and to fully understand the interplay between electronic and ionic transport in OMIECs, OECTs serve as a starting point owing to the well-studied Bernard–Malliaras mode that describes OECT operation. While the semi-quantitative nature of this classic model is still of relevance, its ability to perform quantitative predictions is typically restricted to low polarization voltages and low operating frequencies. Recently, this model has become the foundation for more detailed descriptions of device operation, which build upon a more accurate understanding of charge-transport mechanisms and how they are affected by the microstructural features of the OMIECs. For example, in OMIECs—as in most organic semiconductors—the lack of long-range order limits the electronic charge carriers to nanometric domains such as crystallites and/or along the backbone of the polymer chains and thermally activated hopping is needed for inter-chain and inter-domain transport.[1] The quantum mechanical description of these tunneling events indicates a strong dependence of the hopping rate on the distance and the relative energy between hopping locations, this rate being generally worse in systems characterized by less dense sites—both in terms of space and energy distributions. Given the stochastic assortment of hopping energies and distances, whose statistical distribution is enclosed in the density of states (DOS) of the semiconductor, not all charges exhibit the same mobility.[97,98] In OMIEC-based devices such as OECTs, where the charge-carrier concentration gradually increases with increasing polarization, holes (or electrons) tend to first populate low energy sites that are sparser, where the hopping rate is lower, to then access more densely packed states at higher energies, characterized by higher mobilities.[97,98] As the DOS is incrementally filled beyond the region of optimal transport, the available states tend to become sparse again, thus determining an inflection in the increase of the conductivity. Indeed, compared to conventional FETs, the charge density reached in OECTs is much larger and therefore more band filling may be noticeable. Friedlein et al. argue that, for this reason, the polarization-controlled change in conductivity of the OECT channel—also known as transconductance—displays a characteristic bell-shape,[91] although other authors suggest that this phenomenon can originate from a gate-dependent contact resistance.[99] In any case, this non-monotonic trend of the transconductance has important consequences on the operation of OECTs in real-life scenarios, particularly in biosensing applications, where it is desirable for the device to be operated in the voltage range that maximizes this figure of merit.[91,100]

If we also take into account that ion motion within the polymer bulk may heterogeneously alter the microstructure of the OMIECs, thus affecting the energy landscape of the

semiconductor (i.e., the DOS), the description just provided for the charge-density-dependent mobility becomes more complicated.[101–104] In a general sense, investigating the contribution of ionic transport to the OMIEC tunable conductivity is a non-trivial task. Ion-transport models are not only dependent on the OMIECs properties, but also on the nature of the ionic species, as well as on the characteristics of the liquid or solid electrolyte matrix. While electrical and optical measurements can be used to deconvolute the electronic and ionic contributions, and thus selectively probe ion transport, they generally require either dedicated experimental apparatuses or complex data interpretation based on equivalent circuit models.[105,106] For a long time, OECTs were considered an instrumental testbed for decoupling ion and electron transport in OMIECs, following the general depiction of ionic motions provided by the Bernard–Malliaras model, where lateral ionic drift and/or diffusion are not contemplated. The Bernard–Malliaras representation has been recently improved with more sophisticated 2D drift–diffusion models, which account for ion and hole conductions both along the channel of the OECT and its normal axis.[100,107–109] Furthermore, increasing consideration is being devoted to quantifying and modeling contact resistance effects in OECTs, again with the goal of understanding how the energetic and microstructural features of OMIECs affect charge injection and transport in the material.[99,109–111]

As evident from the above discussion, when reviewing the electrical tuning of the conductivity in OMIECs it is inevitable to refer continuously to the OECT. This pervasive electronic device is in fact a unique tool for investigating these charge modulation phenomena, while simultaneously being the device platform that most benefits of these fundamental studies. Nonetheless, two new families of OMIEC-based devices that exploit the electrically tunable conductivity of this class of materials have very recently emerged. OMIEC-based memory devices on one side, and microwave metadevices on the other. These promising technologies take the structure and the general idea of the OECT to tackle application scenarios that, until very recently, were the prerogative of inorganic or carbon-based non-organic materials. Recent notable examples of OMIEC-based neuromorphic devices present architectures that are very similar to those of OECTs. These three-terminal devices comprise a pre-synaptic and a post-synaptic electrode, both made with OMIECs and electrically coupled through an electrolyte, which are fundamentally equivalent to the gate and source–drain electrodes in OECTs, respectively. When a voltage is applied to the pre-synaptic electrode, the conductive state of the post-synaptic electrode is "written"—that is, fixed—at a predetermined state, and subsequently measured—or "read"—by two lateral electrodes. Unlike what happens in transistors, where the measurement of the source–drain current and the biasing of the device occur simultaneously, in these memristive devices the "write" and "read" phases are temporally separated. Because of their volumetric capacitance and mixed-transport characteristics, OMIECs are in fact able to store and stabilize large amounts of electronic charge, which can be used to achieve fine conductance tuning over a wide dynamic range, operating at relatively high switching speeds and low power.[5,112,113] Besides the notable performances of these organic devices even when compared to other memristor technologies, these objects also bear a remarkable potential toward the implementation of artificial neural networks that can potentially integrate with living matter.[114]

The tunable conductivity in a common OMIEC was also used to actively reconfigure conventional microwave structures and metasurfaces operating in the sub-5 GHz as recently demonstrated in recent work by Bonacchini et al.[115] Even in this case, the device structure bears many analogies to that of common OECTs, where a static or quasi-static potential is used to bias the device and tune the volumetric charge density of the OMIEC. The mobile free carriers in the semiconductor are then able to screen or dampen the high-frequency current oscillations that are generated within the metallic resonant structures by the impinging electromagnetic fields. In this configuration, the large variations in conductivity effectively tune the complex permittivity of the OMIEC throughout its volume, thus altering the response of these photonic devices with performances that are comparable to other state-of-the-art tuning strategies based on free-charge carrier modulation. In fact, with respect to other similar approaches based on either lumped elements (e.g., varactor and pin diodes), or materials such as chemical vapor deposited graphene and III-V compound semiconductors, the relatively lower charge-carrier mobility in OMIECs is likely compensated by the extremely large charge modulations, which affect the entire volume of the tuning element rather than a 2D layer. These results bear implications for both the advancement of organic electronic materials and of metadevices at large. A thorough microwave investigation of these materials has never been undertaken, and it could provide new important insight on the charge-transport properties of these polymer systems. Moreover, unlike other tuning strategies, this OMIEC-based approach allows the fabrication of metadevices on virtually any substrate, including flexible and biocompatible ones, with cost-effective and mass-scalable fabrication techniques. These advantages could prove useful toward the development of new wireless bioelectronic interfaces and enhance the pervasiveness of large-area metadevice technologies.[116]

Another promising yet relatively unexplored approach to tune the conductivity of OMIECs is via the absorption of photons leading to form electron–hole pairs, thereby increasing the charge density and hence the conductivity in the material. The physics of photostimulation in organic materials, along with its use in organic optoelectronic technologies, is an ongoing subject of study, which has been covered by excellent review articles.[117–119] Interestingly, it has been shown that conventional hydrophobic organic semiconductors are able to support charge photogeneration and extraction even when immersed into aqueous environments. As discussed in Section 3.3, these developments have led to remarkable progress in the fields of bioelectronics—where organic photoactive films and nanostructures are used to elicit biological activity in living cells and tissues—and of photocatalysis. For example, organic electrolytic photocapacitors operating as photodiodes in water have been shown by the groups of Lanzani and Głowacki.[51,54,120] From a fundamental point of view, it is yet unclear whether hydrated OMIECs are susceptible to similar optoelectronic processes, and whether phenomena like exciton generation and separation can occur within these mixed conductors, either by means of electrical fields or through the realization of heterojunctions.

For this reason, further attention should be dedicated to exploring this dynamic tuning strategy in OMIECs.

4.3. Color

4.3.1. Chemically Tuned Coloration

In OMIECs, optical changes in the material result from the introduction of mid-bandgap energetic states to the doping (oxidation or reduction) of the material. Key to the successful use of these materials in electrochromic devices is the ability to dope them over a large range in the bulk. ECDs are one of the main applications that take advantage of the coloring/bleaching behavior of OMIECs. The molecular tunability of conjugated polymers has been widely utilized to afford a multitude of colors. Noteworthy is the work by Prof. John Reynolds (**Figure 5**), who, through fine tuning of the conjugated backbones, has demonstrated that: i) the entire color wheel can be designed and synthesized, ii) electrochromic polymers (ECPs) can be readily solution-processed into large-area solid-state electrochromic devices, and iii) the utility of such devices in full-color bistable displays, energy-saving tinted windows, and dimmable glasses, goggles, and visors.[3,121] To afford a myriad of colorations as well as neutral gray, the donor–acceptor approach is mainly utilized to tailor the absorption spectra of desired polymers as illustrated in Figure 5. Common backbone engineering strategies include tuning the core heterocycle choice (e.g., PEDOT), controlling the electron-rich/poor character, modulating the steric strain, as well as copolymerization.[122,123]

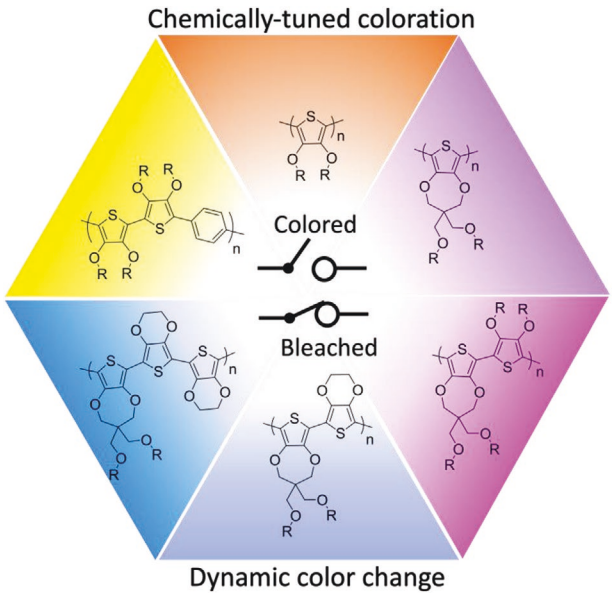

Figure 5. Illustration of color control in OMIECs through both chemical and dynamic tuning. Backbone and sidechain engineering strategies, a multitude of colors can be synthesized and processed into films. Such films can controllably exhibit a colored or bleached state (i.e., electrochromism) upon electronically controlled ionic insertion and expulsion. In the chemical structures, R stands for alkyl chains which can be either linear or branched. Figure prepared based on data and information in refs. [3], [124], and [125].

Different chromophores can also be blended to afford hybrid colors following the classical color mixing theory. Furthermore, the appearance of a polymer film is impacted by other solid-state properties such as crystallinity and molecular anisotropy. Electrochromics being one of the more mature OMIEC-based technologies to date, key lessons can be borrowed by other applications both from a materials and device viewpoint. However, since ECDs are commonly large (in size) and do not necessarily need to operate at high speeds (switching times of several seconds are often acceptable), charge kinetics ought to be carefully considered when borrowing electrochromic material systems for other purposes. Some of existing challenges in designing new ECPs include color complementarity (chromophore design) and environmental stability,[9] two aspects from which other technologies discussed herein can benefit.

Though not as intuitive as it is the case for backbone engineering, sidechains also play a role in the coloration of polymer OMIECs. The exemplar structure PAT, once flanked with branched and bulky sidechains such as ethylhexyloxy at the 3 and 4 positions, appears orange in its neutral state. The color can be redshifted by replacing the branched sidechains with the hexagonally linked and more electron-rich ethylenedioxy to form PEDOT, which forms a blue film. This substitution tunes the ionization potential and affords an energy bandgap of 1.6 eV. In the case of 3,4-propylenedioxythiophene (ProDOT) and dioxythiophene (DOT) and corresponding derivatives, sidechain branching has also shown to significantly tune the coloration of these EC polymers.[126] Further design strategies on utilizing sidechains to control color have been reviewed more extensively elsewhere.[9,121] For the current discussion, the readers are reminded that when designing/selecting sidechains in OMIECs, their impact on film formation, crystallization, and resulting absorption properties should be considered according to intended applications.

Chemical dopants can be introduced into OMIECs to modify their coloration. For instance, electron-rich chemical dopants such as 4(1,3 dimethyl-2,3-dihydro-1H-benzoimidazol-2-yl) phenyl)dimethylamine (N-DMBI)[127] or amines[18] can be used to donate electrons into electron-deficient OMIECs. The injection of electrons into the LUMO of n-type OMIECs increases the optical bandgap of the OMIEC, thereby bleaching the absorption of the backbone. Simultaneously, polarons are formed with energy levels within the bandgap, which absorb photons at lower energies in the IR. This results in an increase in transparency of the OMIEC in the visible range. On the other hand, electron-deficient dopants such as F4TCNQ can be used to extract electrons from the HOMO of low ionization potential, typically p-type OMIECs. This also increases the optical bandgap of the OMIEC and forms positive polarons. Conversely, amines have been utilized to inject electrons into the highly depleted HOMO of PEDOT:PSS. This results in the reverse effect, the de-doping of the OMIEC, thereby turning the polymer from an almost transparent film into darker shades of blue in the visible region.[18] Controlling the transparency of OMIECs in the visible region and their absorption in the IR enables transparent yet thermally insulating windows. One could also envision that by controlling the dopant concentration in OMIEC solutions, different colored inks can be deposited using a single OMIEC.

4.3.2. Dynamically Tuned Coloration

During the electrochemical (and more generally chemical) doping of OMIECs, the color of the polymeric film changes, thereby doping the polymeric film (as illustrated in Figure 5). These changes can be induced by applying an electric potential on the OMIEC or via redox-active molecules that inject charges into the bulk of the polymer. Electrically induced color changes have led to electrochromic devices that can be used for smart windows.[128] The change in color is associated with the formation of the polaron (charge defect) and bipolaron in the film. The extent of color changes is a direct consequence of doping effectiveness. Spectroelectrochemical experiments in the visible,[13] NIR, and UV regions allow tracking the doping level in situ by analyzing changes in the absorption spectra, during electrochemical charging and discharging. The formation of the polaron and the bipolaron is usually associated with quenching of the main visible peak of the pristine polymer and the formation of another peak in the NIR, and the spectra present isosbestic points.

Another approach to change the perceived color of conjugated polymers is to control the film thickness at the nanoscale. Jonsson and co-workers proposed this novel method by depositing PEDOT:tosylate on a metallic surface, controlling film thickness by varying the UV exposure time for vapor film polymerization.[129] This tunability of structural color through light manipulation in conductive polymers has made the materials appealing for optical coatings or multifunctional displays.

4.4. Volume

4.4.1. Tuning Volume Chemically

The ability of a polymer material to accommodate ionic species into its bulk is an indicator of its performance in OMIEC devices. Intuitively, a volumetric change will occur in the polymer film during the charging and discharging of the polymer film to compensate for the ionic flux which compensates the change in electronic carrier density. As previously hinted, a balance between how much electrolyte embeds into the film, the induced bulky swelling, and resulting property changes constitutes the puzzle of how a given OMIEC functions. Relating the sidechain choice to ionic conductivity and volumetric changes in a given electrolyte should thus always be evaluated when benchmarking novel materials. On this front, sidechains' linkage position away from the backbone,[130] their hydrophilicity,[22,131] and length[132] have been shown to impact the swelling of the polymer film, and hence, electrochemical performance of the device. Since these sidechain engineering strategies are also known to impact polymer crystallinity and electronic conductivity, we believe this is one of the areas of study for OMIECs that deserve more attention to drive the field forward. Fortunately, several in situ characterization techniques (e.g., moving front experiments, spectroelectrochemistry, X-ray crystallography)[133] have recently shown that these properties can be deconvoluted thus guiding new material designs.

4.4.2. Changing Volume Dynamically

OMIECs oxidation and reduction processes can cause significant changes in the volume of the polymer. The migration of the charged species inside the bulk of the OMIECs when external stimuli are applied causes the polymer to swell and, as the process is reversed, shrink. The expansion or contraction movements of the material can be linear, volumetric, or a bending movement.[134] Despite working at the low voltages (<1 V), electrochemically driven changes occur up to 40% for reversible OMIECs devices in the out of plane direction.

The reversible nature of the shrinking and swelling characteristic of the changes in volume, light weight, as well as the biocompatibility of the materials, allow OMIECs to be excellent candidates to be used as actuators mimicking human muscle. Electrochemically triggered OMIECs-based actuators are commonly used for many applications, from the biomedical field (as they work in aqueous at room-temperature environment, as the body fluids) to soft robotics.[135] During the actuation process, many different phenomena explain the reversible changes in volume concur ions and solvent exchange between the polymer and the electrolyte, as well as electrostatic repulsion between similarly charged backbones and conformational changes of the latter. Due to the slow kinetics of ion uptake, OMIECs actuators are relatively slow (maximum switching speed between oxidized and reduced states is 1 Hz for films 1 µm thick).[135] McCulloch and co-workers showed that reducing the length of polymer sidechains allows the shorter chains to fill the voids between polymeric chains, thus preventing ion intercalation and reducing water intake, thus resulting in a smaller volume swelling.[136] A way to increase the volume expansion up to 300% was found by Berggren and co-workers, by designing structures that facilitate the intercalation of hydrated ions into the OMIEC bulk.[137] In their work, carbon monofilaments were coated with the OMIEC, promoting the OMIEC's transition between solid state and gel phase when oxidation-reduction potentials are applied.

In addition to electrical stimulation, volumetric swelling of OMIECs can also be achieved by faradaic charge transfer reactions while immersed in an aqueous electrolyte. For instance, electrochemical actuators can be powered by OMIECs functionalized with enzymes to catalyze the reaction of metabolites such as glucose, enabling self-powered artificial muscles.[47] Harvesting energy from the environment to power soft actuators opens potential venues in smart stimuli-responsive soft robots and microfluidic valves.

4.5. Modulus

4.5.1. Tuning the Modulus Chemically

Though organic materials are commonly considered "soft" compared to inorganics, imparting mechanical deformability in conjugated polymer thin films remains challenging. Engineering approaches are still required in order to mimic the flexibility and stretchability as found in nature (e.g., human skin). The key challenge is to design materials that combine mechanical deformability with electronic performance. The backbone

engineering strategies we discussed above for OMIECs, though beneficial to the electronic conduction, tend to yield highly crystalline and brittle polymers that are not suitable for applications such as actuators and bioconformable electronics. Currently, we find that little has been done on designing and processing intrinsically deformable OMIECs, in part due to the widespread use of PEDOT:PSS which is typically softened using additives.[21,138,139] The study of mechanical properties in OMIECs is thus regarded as a research opportunity to enable electronic devices that can conform with biological tissues or functional as soft actuators. For instance, conjugation break spacers have been heavily studied and copolymerization of fully conjugated blocks with spacer-bearing blocks are well understood in FETs. We envision that these approaches will translate well to polymer OMIECs along with other engineering approaches such as nanoconfinement and molecular additives used to tune the mechanical properties.[21,140–144]

Similar to most properties of OMIECs, control of the morphology and nanoscale interactions of OMIECs can heavily influence mechanical properties. In polymeric OMIECs, mechanical properties such as modulus, breaking strength, and elastic limit are intimately linked to the size, distribution, and amount of crystalline aggregates in the material. For example, controlling these aggregates has led to the development of seemingly "rigid" (i.e., high modulus) polymer semiconductors that display remarkable flexibility and maintain electronic transport properties by inducing nanoconfinement of the polymer and reducing aggregate size.[24] These developments have long-reaching applications in biosensing, flexible thermoelectrics, and even artificial skin.[25] This versatility further highlights that understanding material microstructure is not only of fundamental interest, but is also of immense practical importance, as microstructure impacts properties seemingly as disparate as electronic and mechanical properties. Such complexity in the microstructure of OMIECs thus complicates the fundamental understanding of device operation. During OMIEC operation in electrochemical transistor applications for example, significant volume expansion occurs concomitant with disruption to the ordered regions due to penetration of ions into the bulk during the volumetric charging process.[26] Furthermore, the exact nature of interaction between penetrating ions and the OMIEC is poorly understood and perhaps beyond the scope of this perspective. For a detailed overview on the current understanding of microstructural changes during device operation, readers are pointed to a recent review by Wu et al.[28]

5. Closing Remarks

The ability to simultaneously control the ionic, electronic, and chemical properties of OMIECs throughout the bulk renders them a multifunctional class of materials. For instance, a single MIEC polymer has been utilized as a sensing electrode, an OECT channel material, an energy-storage electrode, and electrochemical actuators proving the potential of OMIECs to enable the fabrication of a fully autonomous intelligent system that utilizes a single material fashioned into specific varied geometries for different device functions. Furthermore, such multifunctionality of OMIECs promises a circular economy of organic electronic devices. At the device's end of life, the functional OMIEC can be recovered and repurposed for a new device (e.g., a battery electrode into an OECT channel). Judicious design of sidechains can enable the dissolution of the OMIEC in solvents orthogonal to their operational electrolyte, enabling the selective recovery of OMIECs. With increased interest in understanding biospheres (soil, water, and air monitoring) and biological systems (agriculture and healthcare), materials that are designed to interface seamlessly with organic and aqueous environments are desirable. The ability to derive organic precursors for the synthesis of OMIECs from naturally occurring sources as well as their ease in solution processibility may allow OMIECs to aid in sustainability efforts and the progress to achieving a circular economy of electronic devices.

Desired properties can be achieved during initial synthesis and processing where chemical design of the conjugated backbone, sidechains, additives, processing solvents, and other conditions provide several degrees of freedom to influence the OMIECs' chemistry and morphology. These parameters, in addition to the existing parameters of conventional device design such as device geometry, provide almost infinite possibilities in device functionalities. Furthermore, these properties can be dynamically tuned via external stimuli such as electrical fields and chemical species, allowing the OMIEC to respond to a variety of environmental inputs and transduce these into outputs of disparate physical and chemical natures.

While organic synthesis provides an almost infinite toolbox for designing OMIECs from their chemical structures all the way to morphology, understanding how backbone and sidechain design, additives, and processing methods influence polymer morphology, and hence second-order properties, remains an open challenge in the field. Understanding these structure–function relationships is imperative for designing high-performance OMIEC-based devices. Additionally, it is important to understand how OMIEC structure and properties change dynamically in response to external stimuli. These can be achieved by in-operando measurements such as in situ electrochemical grazing-incidence wide-angle X-ray dcattering and spectroelectrochemistry which illuminate how the microstructure and optical properties of OMIECs change under applied voltages respectively. We envision that more in situ techniques will be developed in future to probe other combinations of input stimuli and OMIEC property changes to drive deeper understanding of OMIEC operation under dynamic conditions. Insights from these in situ experiments would then inform design criteria for the synthetic design of chemical structure and morphology of OMIECs.

The gargantuan effort to design OMIECs, understand their structure–property relationships, understand how these properties modulate in response to external stimuli, and strategically utilize OMIECs for various sensing, logic, actuation, energy harvesting/storage, and communication applications requires cross-disciplinary teams of chemists, physicists, material scientists, as well as bio-, chemical, electronic, computational, and mechanical engineers. We hope that this perspective highlights the potential of OMIECs in addressing salient challenges in society such as energy, sustainability, healthcare, and the Internet of Things.

Acknowledgements

S.T.M.T. and A.S. gratefully acknowledge financial support from the National Science Foundation, CBET Award# 1804915, DMR Award# 1808401, and from the Stanford Graduate Fellowship (Chevron Fellowship). A.G. acknowledges support from a postdoctoral fellowship from the Geballe Laboratory for Advanced Materials (GLAM) at Stanford University. G.E.B. gratefully acknowledges support from the European Union's Horizon 2020 research and innovation programme under the Marie Skłodowska-Curie grant agreement No. 838799 – LEAPh. T.J.Q. and G.S.L. acknowledge the support from the National Science Foundation Graduate Research Fellowship Program under grant DGE-1656518.

Conflict of Interest

The authors declare no conflict of interest.

Keywords

bioelectronics, conjugated polymers, mixed conductors, organic electronics

Received: December 21, 2021
Revised: February 7, 2022
Published online: April 18, 2022

[1] B. D. Paulsen, K. Tybrandt, E. Stavrinidou, J. Rivnay, *Nat. Mater.* **2020**, *19*, 13.
[2] J. Rivnay, S. Inal, A. Salleo, R. M. Owens, M. Berggren, G. G. Malliaras, *Nat. Rev. Mater.* **2018**, *3*, 17086.
[3] P. M. Beaujuge, J. R. Reynolds, *Chem. Rev.* **2010**, *110*, 268.
[4] D. Melling, J. G. Martinez, E. W. H. Jager, *Adv. Mater.* **2019**, *31*, 1808210.
[5] Y. van de Burgt, A. Melianas, S. T. Keene, G. Malliaras, A. Salleo, *Nat. Electron.* **2018**, *1*, 386.
[6] A. Gumyusenge, A. Melianas, S. T. Keene, A. Salleo, *Annu. Rev. Mater. Res.* **2021**, *51*, 47.
[7] T. Someya, Z. Bao, G. G. Malliaras, *Nature* **2016**, *540*, 379.
[8] F. Torricelli, D. Z. Adrahtas, Z. Bao, M. Berggren, F. Biscarini, A. Bonfiglio, C. A. Bortolotti, C. D. Frisbie, E. Macchia, G. G. Malliaras, I. McCulloch, M. Moser, T.-Q. Nguyen, R. M. Owens, A. Salleo, A. Spanu, L. Torsi, *Nat. Rev. Methods Primers* **2021**, *1*, 66.
[9] X. Li, K. Perera, J. He, A. Gumyusenge, J. Mei, *J. Mater. Chem. C* **2019**, *7*, 12761.
[10] L. Groenendaal, F. Jonas, D. Freitag, H. Pielartzik, J. R. Reynolds, *Adv. Mater.* **2000**, *12*, 481.
[11] X. Luo, H. Shen, K. Perera, D. T. Tran, B. W. Boudouris, J. Mei, *ACS Macro Lett.* **2021**, *10*, 1061.
[12] A. Giovannitti, C. B. Nielsen, D.-T. Sbircea, S. Inal, M. Donahue, M. R. Niazi, D. A. Hanifi, A. Amassian, G. G. Malliaras, J. Rivnay, I. McCulloch, *Nat. Commun.* **2016**, *7*, 13066.
[13] D. Moia, A. Giovannitti, A. A. Szumska, I. P. Maria, E. Rezasoltani, M. Sachs, M. Schnurr, P. R. F. Barnes, I. Mcculloch, J. Nelson, *Energy Environ. Sci.* **2019**, *12*, 1349.
[14] J. Surgailis, A. Savva, V. Druet, B. D. Paulsen, R. Wu, A. Hamidi-Sakr, D. Ohayon, G. Nikiforidis, X. Chen, I. McCulloch, J. Rivnay, S. Inal, *Adv. Funct. Mater.* **2021**, *31*, 2010165.
[15] X. Chen, A. Marks, B. D. Paulsen, R. Wu, R. B. Rashid, H. Chen, M. Alsufyani, J. Rivnay, I. McCulloch, *Angew. Chem., Int. Ed.* **2021**, *60*, 9368.
[16] I. P. Maria, B. D. Paulsen, A. Savva, D. Ohayon, R. Wu, R. Hallani, A. Basu, W. Du, T. D. Anthopoulos, S. Inal, J. Rivnay, I. McCulloch, A. Giovannitti, *Adv. Funct. Mater.* **2021**, *31*, 2008718.
[17] S. Che, L. Fang, *Chem* **2020**, *6*, 2558.
[18] S. T. Keene, T. P. A. van der Pol, D. Zakhidov, C. H. L. Weijtens, R. A. J. Janssen, A. Salleo, Y. van de Burgt, *Adv. Mater.* **2020**, *32*, 2000270.
[19] D. Kiefer, A. Giovannitti, H. Sun, T. Biskup, A. Hofmann, M. Koopmans, C. Cendra, S. Weber, L. J. Anton Koster, E. Olsson, J. Rivnay, S. Fabiano, I. McCulloch, C. Müller, *ACS Energy Lett.* **2018**, *3*, 278.
[20] C. Y. Yang, Y. F. Ding, D. Huang, J. Wang, Z. F. Yao, C. X. Huang, Y. Lu, H. I. Un, F. D. Zhuang, J. H. Dou, C. an Di, D. Zhu, J. Y. Wang, T. Lei, J. Pei, *Nat. Commun.* **2020**, *11*, 3292.
[21] J. W. Onorato, C. K. Luscombe, *Mol. Syst. Des. Eng.* **2019**, *4*, 310.
[22] L. Q. Flagg, C. G. Bischak, J. W. Onorato, R. B. Rashid, C. K. Luscombe, D. S. Ginger, *J. Am. Chem. Soc.* **2019**, *141*, 4345.
[23] A. Giovannitti, D.-T. Sbircea, S. Inal, C. B. Nielsen, E. Bandiello, D. A. Hanifi, M. Sessolo, G. G. Malliaras, I. McCulloch, J. Rivnay, *Proc. Natl. Acad. Sci. USA* **2016**, *113*, 12017 LP.
[24] J. Xu, S. Wang, G. J. N. Wang, C. Zhu, S. Luo, L. Jin, X. Gu, S. Chen, V. R. Feig, J. W. F. To, S. Rondeau-Gagné, J. Park, B. C. Schroeder, C. Lu, J. Y. Oh, Y. Wang, Y. H. Kim, H. Yan, R. Sinclair, D. Zhou, G. Xue, B. Murmann, C. Linder, W. Cai, J. B. H. Tok, J. W. Chung, Z. Bao, *Science* **2017**, *355*, 59.
[25] A. Chortos, J. Liu, Z. Bao, *Nat. Mater.* **2016**, *15*, 937.
[26] R. Giridharagopal, L. Q. Flagg, J. S. Harrison, M. E. Ziffer, J. Onorato, C. K. Luscombe, D. S. Ginger, *Nat. Mater.* **2017**, *16*, 737.
[27] M. Matta, R. Wu, B. D. Paulsen, A. J. Petty, R. Sheelamanthula, I. McCulloch, G. C. Schatz, J. Rivnay, *Chem. Mater.* **2020**, *32*, 7301.
[28] R. Wu, M. Matta, B. D. Paulsen, J. Rivnay, *Chem. Rev.* **2022**, *122*, 4493.
[29] B. Russ, A. Glaudell, J. J. Urban, M. L. Chabinyc, R. A. Segalman, *Nat. Rev. Mater.* **2016**, *1*, 16050.
[30] J. Kawahara, P. A. Ersman, I. Engquist, M. Berggren, *Org. Electron.* **2012**, *13*, 469.
[31] F. Hu, Y. Xue, J. Xu, B. Lu, *Front. Rob. AI* **2019**, *6*, 114.
[32] M. Jakešová, T. A. Sjöström, V. Đerek, D. Poxson, M. Berggren, E. D. Głowacki, D. T. Simon, *npj Flexible Electron.* **2019**, *3*, 14.
[33] B. Rivkin, C. Becker, F. Akbar, R. Ravishankar, D. D. Karnaushenko, R. Naumann, A. Mirhajivarzaneh, M. Medina-Sánchez, D. Karnaushenko, O. G. Schmidt, *Adv. Intell. Syst.* **2021**, *3*, 2000238.
[34] O. Kanoun, A. Bouhamed, R. Ramalingame, J. R. Bautista-Quijano, D. Rajendran, A. Al-Hamry, *Sensors* **2021**, *21*, 341.
[35] R. D. Rodriguez, S. Shchadenko, G. Murastov, A. Lipovka, M. Fatkullin, I. Petrov, T. H. Tran, A. Khalelov, M. Saqib, N. E. Villa, V. Bogoslovskiy, Y. Wang, C. G. Hu, A. Zinovyev, W. Sheng, J. J. Chen, I. Amin, E. Sheremet, *Adv. Funct. Mater.* **2021**, *31*, 2008818.
[36] A. Giovannitti, R. B. Rashid, Q. Thiburce, B. D. Paulsen, C. Cendra, K. Thorley, D. Moia, J. T. Mefford, D. Hanifi, D. Weiyuan, M. Moser, A. Salleo, J. Nelson, I. McCulloch, J. Rivnay, *Adv. Mater.* **2020**, *32*, 1908047.
[37] M. Ghittorelli, L. Lingstedt, P. Romele, N. I. Cračiun, Z. M. Kovács-Vajna, P. W. M. Blom, F. Torricelli, *Nat. Commun.* **2018**, *9*, 1441.
[38] S. T. Keene, D. Fogarty, R. Cooke, C. D. Casadevall, A. Salleo, O. Parlak, *Adv. Healthcare Mater.* **2019**, *8*, 1901321.
[39] C. Pitsalidis, A. M. Pappa, M. Porel, C. M. Artim, G. C. Faria, D. D. Duong, C. A. Alabi, S. Daniel, A. Salleo, R. M. Owens, *Adv. Mater.* **2018**, *30*, 1803130.
[40] X. Zeng, K. Qu, A. Rehman, *Acc. Chem. Res.* **2016**, *49*, 1624.
[41] X. Strakosas, M. Bongo, R. M. Owens, *J. Appl. Polym. Sci.* **2015**, *132*, 41735.

[42] S. Pirsa, *Mater. Sci. Eng.: Concepts, Methodol., Tools, Appl.* **2017**, *1–3*, 543.
[43] A. Koklu, D. Ohayon, S. Wustoni, A. Hama, X. Chen, I. McCulloch, S. Inal, *Sens. Actuators, B* **2021**, *329*, 129251.
[44] G. Méhes, A. Roy, X. Strakosas, M. Berggren, E. Stavrinidou, D. T. Simon, *Adv. Sci.* **2020**, *7*, 2000641.
[45] S. T. M. Tan, S. Keene, A. Giovannitti, A. Melianas, M. Moser, I. McCulloch, A. Salleo, *J. Mater. Chem. C* **2021**, *9*, 12148.
[46] S. T. M. Tan, A. Giovannitti, A. Melianas, M. Moser, B. L. Cotts, D. Singh, I. McCulloch, A. Salleo, *Adv. Funct. Mater.* **2021**, *31*, 2010868.
[47] F. Mashayekhi Mazar, J. G. Martinez, M. Tyagi, M. Alijanianzadeh, A. P. F. Turner, E. W. H. Jager, *Adv. Mater.* **2019**, *31*, 1901677.
[48] D. Ji, T. Li, J. Liu, S. Amirjalayer, M. Zhong, Z. Y. Zhang, X. Huang, Z. Wei, H. Dong, W. Hu, H. Fuchs, *Nat. Commun.* **2019**, *10*, 12.
[49] X. Huang, D. Ji, H. Fuchs, W. Hu, T. Li, *ChemPhotoChem* **2020**, *4*, 9.
[50] D. Ghezzi, M. R. Antognazza, R. Maccarone, S. Bellani, E. Lanzarini, N. Martino, M. Mete, G. Pertile, S. Bisti, G. Lanzani, F. Benfenati, *Nat. Photonics* **2013**, *7*, 400.
[51] D. Rand, M. Jakešová, G. Lubin, I. Vėbraitė, M. David-Pur, V. Đerek, T. Cramer, N. S. Sariciftci, Y. Hanein, E. D. Głowacki, *Adv. Mater.* **2018**, *30*, 1707292.
[52] B. Kolodziejczyk, C. H. Ng, X. Strakosas, G. G. Malliaras, B. Winther-Jensen, *Mater. Horiz.* **2018**, *5*, 93.
[53] J. F. Maya-Vetencourt, D. Ghezzi, M. R. Antognazza, E. Colombo, M. Mete, P. Feyen, A. Desii, A. Buschiazzo, M. Di Paolo, S. Di Marco, F. Ticconi, L. Emionite, D. Shmal, C. Marini, I. Donelli, G. Freddi, R. Maccarone, S. Bisti, G. Sambuceti, G. Pertile, G. Lanzani, F. Benfenati, *Nat. Mater.* **2017**, *16*, 681.
[54] M. Jakešová, M. Silverå Ejneby, V. Đerek, T. Schmidt, M. Gryszel, J. Brask, R. Schindl, D. T. Simon, M. Berggren, F. Elinder, E. D. Głowacki, *Sci. Adv.* **2019**, *5*, eaav5265.
[55] M. Silverå Ejneby, M. Jakešová, J. J. Ferrero, L. Migliaccio, I. Sahalianov, Z. Zhao, M. Berggren, D. Khodagholy, V. Đerek, J. N. Gelinas, E. D. Głowacki, *Nat. Biomed. Eng.* **2021**, https://doi.org/10.1038/s41551-021-00817-7.
[56] G. Tullii, F. Gobbo, A. Costa, M. R. Antognazza, *Adv. Sustainable Syst.* **2021**, *5*, 2100048.
[57] F. Benfenati, G. Lanzani, *Nat. Nanotechnol.* **2021**, *16*, 1333.
[58] D. Palanker, E. D. Głowacki, D. Ghezzi, *Nat. Nanotechnol.* **2021**, *16*, 1330.
[59] T. Paltrinieri, L. Bondi, V. Đerek, B. Fraboni, E. Daniel Głowacki, T. Cramer, T. Paltrinieri, L. Bondi, B. Fraboni, T. Cramer, V. Đerek, E. D. Głowacki, *Adv. Funct. Mater.* **2021**, *31*, 2010116.
[60] F. Di Maria, F. Lodola, E. Zucchetti, F. Benfenati, G. Lanzani, *Chem. Soc. Rev.* **2018**, *47*, 4757.
[61] R. Wei, M. Gryszel, L. Migliaccio, E. D. Głowacki, *J. Mater. Chem. C* **2020**, *8*, 10897.
[62] F. Milos, G. Tullii, F. Gobbo, F. Lodola, F. Galeotti, C. Verpelli, D. Mayer, V. Maybeck, A. Offenhäusser, M. R. Antognazza, *ACS Appl. Mater. Interfaces* **2021**, *13*, 23438.
[63] J. F. Maya-Vetencourt, G. Manfredi, M. Mete, E. Colombo, M. Bramini, S. Di Marco, D. Shmal, G. Mantero, M. Dipalo, A. Rocchi, M. L. DiFrancesco, E. D. Papaleo, A. Russo, J. Barsotti, C. Eleftheriou, F. Di Maria, V. Cossu, F. Piazza, L. Emionite, F. Ticconi, C. Marini, G. Sambuceti, G. Pertile, G. Lanzani, F. Benfenati, *Nat. Nanotechnol.* **2020**, *15*, 698.
[64] M. Sytnyk, M. Jakešová, M. Litviňuková, O. Mashkov, D. Kriegner, J. Stangl, J. Nebesářová, F. W. Fecher, W. Schöfberger, N. S. Sariciftci, R. Schindl, W. Heiss, E. D. Głowacki, *Nat. Commun.* **2017**, *8*, 91.
[65] S. Bellani, M. R. Antognazza, F. Bonaccorso, S. Bellani, F. Bonaccorso, G. Labs, M. R. Antognazza, *Adv. Mater.* **2019**, *31*, 1801446.
[66] M. Gryszel, E. D. Głowacki, *Chem. Commun.* **2020**, *56*, 1705.
[67] H. Bronstein, C. B. Nielsen, B. C. Schroeder, I. McCulloch, *Nat. Rev. Chem.* **2020**, *4*, 66.
[68] A. Giovannitti, I. P. Maria, D. Hanifi, M. J. Donahue, D. Bryant, K. J. Barth, B. E. Makdah, A. Savva, D. Moia, M. Zetek, P. R. F. Barnes, O. G. Reid, S. Inal, G. Rumbles, G. G. Malliaras, J. Nelson, J. Rivnay, I. McCulloch, *Chem. Mater.* **2018**, *30*, 2945.
[69] M. Heeney, C. Bailey, K. Genevicius, M. Shkunov, D. Sparrowe, S. Tierney, I. McCulloch, *J. Am. Chem. Soc.* **2005**, *127*, 1078.
[70] M. R. Andersson, O. Thomas, W. Mammo, M. Svensson, M. Theander, O. Inganäs, *J. Mater. Chem.* **1999**, *9*, 1933.
[71] D. J. Crouch, P. J. Skabara, M. Heeney, I. McCulloch, D. Sparrowe, S. J. Coles, M. B. Hursthouse, *Macromol. Rapid Commun.* **2008**, *29*, 1839.
[72] I. McCulloch, C. Bailey, M. Giles, M. Heeney, I. Love, M. Shkunov, D. Sparrowe, S. Tierney, *Chem. Mater.* **2005**, *17*, 1381.
[73] Y. Wang, M. D. Watson, *Macromolecules* **2008**, *41*, 8643.
[74] S. T. M. Tan, T. J. Quill, M. Moser, G. Lecroy, X. Chen, Y. Wu, C. J. Takacs, A. Salleo, A. Giovannitti, *ACS Energy Lett.* **2021**, *6*, 3450.
[75] J. F. Ponder Jr, H. Chen, A. M. T. Luci, S. Moro, M. Turano, A. L. Hobson, G. S. Collier, L. M. A. Perdigão, M. Moser, W. Zhang, G. Costantini, J. R. Reynolds, I. McCulloch, *ACS Mater. Lett.* **2021**, *3*, 1503.
[76] R. J. Mortimer, K. R. Graham, C. R. G. Grenier, J. R. Reynolds, *ACS Appl. Mater. Interfaces* **2009**, *1*, 2269.
[77] S. N. Patel, A. M. Glaudell, K. A. Peterson, E. M. Thomas, K. A. O'Hara, E. Lim, M. L. Chabinyc, *Sci. Adv.* **2017**, *3*, e1700434.
[78] D. Ohayon, G. Nikiforidis, A. Savva, A. Giugni, S. Wustoni, T. Palanisamy, X. Chen, I. P. Maria, E. Di Fabrizio, P. M. F. J. Costa, I. McCulloch, S. Inal, *Nat. Mater.* **2020**, *19*, 456.
[79] C. B. Nielsen, A. Giovannitti, D.-T. Sbircea, E. Bandiello, M. R. Niazi, D. A. Hanifi, M. Sessolo, A. Amassian, G. G. Malliaras, J. Rivnay, I. McCulloch, *J. Am. Chem. Soc.* **2016**, *138*, 10252.
[80] M. Moser, A. Savva, K. Thorley, B. D. Paulsen, T. C. Hidalgo, D. Ohayon, H. Chen, A. Giovannitti, A. Marks, N. Gasparini, A. Wadsworth, J. Rivnay, S. Inal, I. McCulloch, *Angew. Chem., Int. Ed.* **2021**, *60*, 7777.
[81] A. Savva, R. Hallani, C. Cendra, J. Surgailis, T. C. Hidalgo, S. Wustoni, R. Sheelamanthula, X. Chen, M. Kirkus, A. Giovannitti, A. Salleo, I. McCulloch, S. Inal, *Adv. Funct. Mater.* **2020**, *30*, 1907657.
[82] D. Kiefer, R. Kroon, A. I. Hofmann, H. Sun, X. Liu, A. Giovannitti, D. Stegerer, A. Cano, J. Hynynen, L. Yu, Y. Zhang, D. Nai, T. F. Harrelson, M. Sommer, A. J. Moulé, M. Kemerink, S. R. Marder, I. McCulloch, M. Fahlman, S. Fabiano, C. Müller, *Nat. Mater.* **2019**, *18*, 149.
[83] R. Noriega, J. Rivnay, K. Vandewal, F. P. V. Koch, N. Stingelin, P. Smith, M. F. Toney, A. Salleo, *Nat. Mater.* **2013**, *12*, 1038.
[84] K. Gu, C. R. Snyder, J. Onorato, C. K. Luscombe, A. W. Bosse, Y.-L. Loo, *ACS Macro Lett.* **2018**, *7*, 1333.
[85] C. Scharsich, R. H. Lohwasser, M. Sommer, U. Asawapirom, U. Scherf, M. Thelakkat, D. Neher, A. Köhler, *J. Polym. Sci., Part B: Polym. Phys.* **2012**, *50*, 442.
[86] R. Steyrleuthner, M. Schubert, I. Howard, B. Klaumünzer, K. Schilling, Z. Chen, P. Saalfrank, F. Laquai, A. Facchetti, D. Neher, *J. Am. Chem. Soc.* **2012**, *134*, 18303.
[87] J. Rivnay, S. Inal, B. A. Collins, M. Sessolo, E. Stavrinidou, X. Strakosas, C. Tassone, D. M. Delongchamp, G. G. Malliaras, *Nat. Commun.* **2016**, *7*, 11287.
[88] S. K. M. Jönsson, J. Birgerson, X. Crispin, G. Greczynski, W. Osikowicz, A. W. Denier van der Gon, W. R. Salaneck, M. Fahlman, *Synth. Met.* **2003**, *139*, 1.
[89] D. A. Mengistie, M. A. Ibrahem, P.-C. Wang, C.-W. Chu, *ACS Appl. Mater. Interfaces* **2014**, *6*, 2292.

[90] A. Håkansson, S. Han, S. Wang, J. Lu, S. Braun, M. Fahlman, M. Berggren, X. Crispin, S. Fabiano, *J. Polym. Sci., Part B: Polym. Phys.* **2017**, *55*, 814.
[91] J. T. Friedlein, R. R. McLeod, J. Rivnay, *Org. Electron.* **2018**, *63*, 398.
[92] S. Inal, G. G. Malliaras, J. Rivnay, *Nat. Commun.* **2017**, *8*, 1767.
[93] I. Sahalianov, S. K. Singh, K. Tybrandt, M. Berggren, I. Zozoulenko, *RSC Adv.* **2019**, *9*, 42498.
[94] S. Wang, M. Ha, M. Manno, C. Daniel Frisbie, C. Leighton, *Nat. Commun.* **2012**, *3*, 1210.
[95] B. D. Paulsen, C. D. Frisbie, *J. Phys. Chem. C* **2012**, *116*, 3132.
[96] C. M. Proctor, J. Rivnay, G. G. Malliaras, *J. Polym. Sci., Part B: Polym. Phys.* **2016**, *54*, 1433.
[97] J. T. Friedlein, J. Rivnay, D. H. Dunlap, I. McCulloch, S. E. Shaheen, R. R. McLeod, G. G. Malliaras, *Appl. Phys. Lett.* **2017**, *111*, 023301.
[98] J. T. Friedlein, S. E. Shaheen, G. G. Malliaras, R. R. McLeod, *Adv. Electron. Mater.* **2015**, *1*, 1500189.
[99] V. Kaphle, S. Liu, A. Al-Shadeedi, C. M. Keum, B. Lüssem, *Adv. Mater.* **2016**, *28*, 8766.
[100] D. Tu, S. Fabiano, *Appl. Phys. Lett.* **2020**, *117*, 080501.
[101] C. Cendra, A. Giovannitti, A. Savva, V. Venkatraman, I. McCulloch, A. Salleo, S. Inal, J. Rivnay, *Adv. Funct. Mater.* **2019**, *29*, 1807034.
[102] B. D. Paulsen, R. Wu, C. J. Takacs, H. G. Steinrück, J. Strzalka, Q. Zhang, M. F. Toney, J. Rivnay, *Adv. Mater.* **2020**, *32*, 2003404.
[103] T. J. Quill, G. LeCroy, A. Melianas, D. Rawlings, Q. Thiburce, R. Sheelamanthula, C. Cheng, Y. Tuchman, S. T. Keene, I. McCulloch, R. A. Segalman, M. L. Chabinyc, A. Salleo, *Adv. Funct. Mater.* **2021**, *31*, 2104301.
[104] L. Q. Flagg, C. G. Bischak, R. J. Quezada, J. W. Onorato, C. K. Luscombe, D. S. Ginger, *ACS Mater. Lett.* **2020**, *2*, 254.
[105] M. Sheliakina, A. B. Mostert, P. Meredith, *Adv. Funct. Mater.* **2018**, *28*, 1805514.
[106] E. Stavrinidou, P. Leleux, H. Rajaona, D. Khodagholy, J. Rivnay, M. Lindau, S. Sanaur, G. G. Malliaras, *Adv. Mater.* **2013**, *25*, 4488.
[107] M. Z. Szymanski, D. Tu, R. Forchheimer, *IEEE Trans. Electron Devices* **2017**, *64*, 5114.
[108] V. Kaphle, P. R. Paudel, D. Dahal, R. K. Radha Krishnan, B. Lüssem, *Nat. Commun.* **2020**, *11*, 2515.
[109] P. R. Paudel, V. Kaphle, D. Dahal, R. K. Radha Krishnan, B. Lüssem, *Adv. Funct. Mater.* **2021**, *31*, 2004939.
[110] F. Bonafè, F. Decataldo, B. Fraboni, T. Cramer, *Adv. Electron. Mater.* **2021**, *7*, 2100086.
[111] A. F. Paterson, H. Faber, A. Savva, G. Nikiforidis, M. Gedda, T. C. Hidalgo, X. Chen, I. McCulloch, T. D. Anthopoulos, S. Inal, *Adv. Mater.* **2019**, *31*, 1902291.
[112] E. J. Fuller, S. T. Keene, A. Melianas, Z. Wang, S. Agarwal, Y. Li, Y. Tuchman, C. D. James, M. J. Marinella, J. J. Yang, A. Salleo, A. A. Talin, *Science* **2019**, *364*, 570.
[113] A. Melianas, T. J. Quill, G. LeCroy, Y. Tuchman, H. V. Loo, S. T. Keene, A. Giovannitti, H. R. Lee, I. P. Maria, I. McCulloch, A. Salleo, *Sci. Adv.* **2020**, *6*, eabb2958.
[114] S. T. Keene, C. Lubrano, S. Kazemzadeh, A. Melianas, Y. Tuchman, G. Polino, P. Scognamiglio, L. Cinà, A. Salleo, Y. van de Burgt, F. Santoro, *Nat. Mater.* **2020**, *19*, 969.
[115] G. E. Bonacchini, F. G. Omenetto, *Nat. Electron.* **2021**, *4*, 424.
[116] Z. Li, X. Tian, C.-W. Qiu, J. S. Ho, *Nat. Electron.* **2021**, *4*, 382.
[117] O. Ostroverkhova, *Chem. Rev.* **2016**, *116*, 13279.
[118] K. J. Baeg, M. Binda, D. Natali, M. Caironi, Y. Y. Noh, *Adv. Mater.* **2013**, *25*, 4267.
[119] C. Wang, X. Zhang, W. Hu, *Chem. Soc. Rev.* **2020**, *49*, 653.
[120] M. R. Antognazza, D. Ghezzi, D. Musitelli, M. Garbugli, G. Lanzani, *Appl. Phys. Lett.* **2009**, *94*, 243501.
[121] C. M. Amb, A. L. Dyer, J. R. Reynolds, *Chem. Mater.* **2011**, *23*, 397.
[122] C. K. Lo, D. E. Shen, J. R. Reynolds, *Macromolecules* **2019**, *52*, 6773.
[123] D. T. Christiansen, A. L. Tomlinson, J. R. Reynolds, *J. Am. Chem. Soc.* **2019**, *141*, 3859.
[124] C. M. Amb, A. L. Dyer, J. R. Reynolds, C. M. Amb, A. L. Dyer, J. R. Reynolds, *Chem. Mater.* **2011**, *23*, 397.
[125] A. L. Dyer, E. J. Thompson, J. R. Reynolds, *ACS Appl. Mater. Interfaces* **2011**, *3*, 1787.
[126] S. L. Pittelli, M. De Keersmaecker, J. F. Ponder Jr, A. M. Österholm, M. A. Ochieng, J. R. Reynolds, *J. Mater. Chem. C* **2020**, *8*, 683.
[127] O. Bardagot, C. Aumaître, A. Monmagnon, J. Pécaut, P.-A. Bayle, R. Demadrille, *Appl. Phys. Lett.* **2021**, *118*, 203904.
[128] C. W. Chang-Jian, E. C. Cho, S. C. Yen, B. C. Ho, K. C. Lee, J. H. Huang, Y. S. Hsiao, *Dyes Pigm.* **2018**, *148*, 465.
[129] S. Chen, S. Rossi, R. Shanker, G. Cincotti, S. Gamage, P. Kühne, V. Stanishev, I. Engquist, M. Berggren, J. Edberg, V. Darakchieva, M. P. Jonsson, *Adv. Mater.* **2021**, *33*, 2102451.
[130] P. Schmode, A. Savva, R. Kahl, D. Ohayon, F. Meichsner, O. Dolynchuk, T. Thurn-Albrecht, S. Inal, M. Thelakkat, *ACS Appl. Mater. Interfaces* **2020**, *12*, 13029.
[131] Y. Wang, E. Zeglio, H. Liao, J. Xu, F. Liu, Z. Li, I. Petruta Maria, D. Mawad, A. Herland, I. McCulloch, W. Yue, *Chem. Mater.* **2019**, *31*, 9797.
[132] M. Moser, L. R. Savagian, A. Savva, M. Matta, J. F. Ponder, T. Cecilia Hidalgo, D. Ohayon, R. Hallani, M. Reisjalali, A. Troisi, A. Wadsworth, J. R. Reynolds, S. Inal, I. McCulloch, *Chem. Mater.* **2020**, *32*, 6618.
[133] B. D. Paulsen, A. Giovannitti, R. Wu, J. Strzalka, Q. Zhang, J. Rivnay, C. J. Takacs, *Small* **2021**, *17*, 2103213.
[134] L. Bay, K. West, P. Sommer-Larsen, S. Skaarup, M. Benslimane, *Adv. Mater.* **2003**, *15*, 310.
[135] H. Stoyanov, M. Kollosche, S. Risse, R. Waché, G. Kofod, *Adv. Mater.* **2013**, *25*, 578.
[136] M. Moser, J. Gladisch, S. Ghosh, T. C. Hidalgo, J. F. Ponder, R. Sheelamanthula, Q. Thiburce, N. Gasparini, A. Wadsworth, A. Salleo, S. Inal, M. Berggren, I. Zozoulenko, E. Stavrinidou, I. McCulloch, *Adv. Funct. Mater.* **2021**, *31*, 2100723.
[137] J. Gladisch, E. Stavrinidou, S. Ghosh, A. Giovannitti, M. Moser, I. Zozoulenko, I. McCulloch, M. Berggren, *Adv. Sci.* **2020**, *7*, 1901144.
[138] V. R. Feig, H. Tran, M. Lee, Z. Bao, *Nat. Commun.* **2018**, *9*, 2740.
[139] S. Savagatrup, E. Chan, S. M. Renteria-Garcia, A. D. Printz, A. V. Zaretski, T. F. O'Connor, D. Rodriquez, E. Valle, D. J. Lipomi, *Adv. Funct. Mater.* **2015**, *25*, 427.
[140] A. Gumyusenge, D. T. Tran, X. Luo, G. M. Pitch, Y. Zhao, K. A. Jenkins, T. J. Dunn, A. L. Ayzner, B. M. Savoie, J. Mei, *Science* **2018**, *362*, 1131.
[141] A. Gumyusenge, X. Luo, H. Zhang, G. M. Pitch, A. L. Ayzner, J. Mei, *ACS Appl. Polym. Mater.* **2019**, *1*, 1778.
[142] S. E. Root, S. Savagatrup, A. D. Printz, D. Rodriquez, D. J. Lipomi, *Chem. Rev.* **2017**, *117*, 6467.
[143] B. Roth, S. Savagatrup, N. V. de los Santos, O. Hagemann, J. E. Carlé, M. Helgesen, F. Livi, E. Bundgaard, R. R. Søndergaard, F. C. Krebs, D. J. Lipomi, *Chem. Mater.* **2016**, *28*, 2363.
[144] S. Savagatrup, A. D. Printz, T. F. O'Connor, A. V. Zaretski, D. J. Lipomi, *Chem. Mater.* **2014**, *26*, 3028.

Siew Ting Melissa Tan earned her bachelor's in engineering in materials science and engineering with a specialization in nanotechnology from Nanyang Technological University, Singapore in 2018 where she was an Agency for Science, Technology and Research scholar, CN Yang scholar, and Koh Boon Hwee scholar. She is currently pursuing a Ph.D. in materials science and engineering at Stanford University with Prof. Alberto Salleo, supported by a Stanford Graduate Fellowship and a National University of Singapore Development Grant. Her Ph.D. work focuses on the fundamental understanding of organic mixed conductors for electrochemical devices, organic transistors, biosensors, and energy-storage devices.

Aristide Gumyusenge received a B.S. in chemistry from Wofford College (2015), a Ph.D. in chemistry from Purdue University (2019), and was the GLAM Postdoctoral Fellow at Stanford University. In 2022, he joined MIT as an Assistant, where he holds the Merton C. Flemings Career Development Professorship. His research interests are in semiconducting polymers, their processing and characterization, and their unique role in future electronics. He has been selected as a PMSE Future Faculty Scholar, the GLAM Postdoctoral Fellow, the MRS Arthur Nowick and Graduate Student Gold Awardee, amongst other recognitions.

Tyler James Quill is a doctoral candidate in the Materials Science and Engineering Department at Stanford University. His research focuses on understanding the structure–property relations in neuromorphic devices and artificial synapses based on organic mixed conductors. He is a National Science Foundation graduate research fellow and a U.S. Department of Energy Office of Science graduate research fellow.

Garrett Swain LeCroy is a Ph.D. candidate at Stanford University working under the supervision of Alberto Salleo. He graduated from Georgia Institute of Technology in 2018 with his B.S. in materials science and engineering. He is interested in fundamental light–matter interactions in disordered semiconductors and uses spectroscopy to study charge-transport properties. He is a National Science Foundation graduate research fellow.

Giorgio E. Bonacchini received his Ph.D. from Politecnico di Milano, working at the Center for Nano Science and Technology of the Istituto Italiano di Tecnologia. He then joined the Silklab at Tufts University, where he developed the first demonstration of microwave metadevices based on organic electrochemical transistors. As of July 2020, he has been a Marie Skłodowska-Curie Actions Global Fellow working in the Salleo Group at Stanford University, where he is studying the optoelectronic properties of organic semiconductors and mixed ion–electron conductors, with a focus on the development of water-gated organic phototransistors and microwave metadevices.

Ilaria Denti received her bachelor's and master's degree in physics at the Universita' degli Studi di Milano. She is currently finishing her Ph.D. in materials engineering at Politecnico di Milano in the laboratory of Prof. Chiara Castiglioni. In 2019, during her Ph.D. she joined the laboratory of Prof. Alberto Salleo as a visiting scholar at Stanford University, where she currently continues her research activity. The main focus of her work is the use of vibrational spectroscopy to characterize the charge defect (i.e., polarons) of doped semiconductive polymers, developing novel setups for in situ characterization.

Alberto Salleo is Professor of Materials Science and Department Chair at Stanford University. He has a Ph.D. in materials science from UC Berkeley and was post-doc, then staff member at Xerox PARC. In 2005 he joined the Materials Science and Engineering Department at Stanford as an Assistant Professor. At Stanford, he won the NSF Career Award, the 3M Untenured Faculty Award, the SPIE Early Career Award, and the Gores Award for Excellence in Teaching, Stanford's highest teaching award. He has been a Clarivate Highly Cited Researcher since 2015 and was elected to the European Academy of Sciences in 2021.